NATIONAL ADVISORY COMMITTEE FOR AERONAUTICS

TECHNICAL NOTE

No. 1873

SUBSONIC TWO-DIMENSIONAL-FLOW CONDITIONS NEAR AN

AIRFOIL DETERMINED BY STATIC PRESSURES

MEASURED AT THE TUNNEL WALL

By Bernard N. Daley and Lillian E. Hanna

Langley Aeronautical Laboratory
Langley Air Force Base, Va.

20000803 209

NACA

Washington

April 1949

AQM00-10-3159

NATIONAL ADVISORY COMMITTEE FOR AERONAUTICS

TECHNICAL NOTE NO. 1873

SUBSONIC TWO-DIMENSIONAL-FLOW CONDITIONS NEAR AN

AIRFOIL DETERMINED BY STATIC PRESSURES

MEASURED AT THE TUNNEL WALL

By Bernard N. Daley and Lillian E. Hanna

SUMMARY

Static pressures existing in the neighborhood of the NACA 66,2-015 and NACA 66,2-215 airfoils in two-dimensional flow were measured at Mach numbers between 0.300 and 0.800 in the Langley rectangular high-speed tunnel. These measurements were made by means of numerous orifices in the model end plate which was fitted flush with the tunnel wall. The investigation was conducted to determine the possibility of obtaining by this method the flow conditions in the region influenced by the model.

The experimental results obtained at low speeds with the NACA 66,2-015 airfoil at an angle of attack of 0° were corrected to a stream Mach number of 0 and were compared with those computed for incompressible flow from theoretical pressure distributions by means of the Cauchy contour integral. Reasonably good agreement was obtained between the theoretically and experimentally determined pressure contours.

By the application of the methods of Prandtl and Ackeret to the flow field, the low-speed flow-field data can be extended for use at subcritical Mach numbers. The flow-field pressures measured at the wall, when judged by their relation to the midspan surface pressures, appeared to be reasonably representative of conditions at the midspan location in the field, except when steep pressure gradients or flow separation were encountered.

INTRODUCTION

Almost all previous theoretical and experimental investigations concerning the flow over airfoils have been aimed at the determination of the pressures on the surfaces of these bodies. These data readily provide useful information concerning the forces experienced by the body, but a knowledge of the flow field about the body would help in the analysis of various high-speed flow phenomena, such as interpretation of schlieren

photographs, study of wind–tunnel constriction, and determination of interference on airplane components placed within the region affected by the wing.

The pressures in the flow field of a bump on a wind–tunnel wall have been obtained (reference 1) by surveying the test region with a small pitot–static tube. In this method, alinement of the tube with the local air stream is difficult and interference with the flow can be introduced. It was believed that measurements of static pressure at the tunnel wall would provide a rapid and reliable means of determining two–dimensional–flow conditions in the field of a model, provided the tunnel–wall boundary layer did not seriously affect the measurements. The purpose of the tests reported herein was to investigate the possibility of measuring flow–field pressures by means of orifices in the tunnel wall and to compare these experimental values with those obtained by theory.

SYMBOLS

α angle of attack of model

c chord of model

p stream static pressure

p_l local static pressure on model surface

p_f local static pressure in flow field of model

P pressure coefficient $\left(\dfrac{p_l - p}{q} \quad \text{or} \quad \dfrac{p_f - p}{q} \right)$

q stream dynamic pressure

M stream Mach number

M_{cr} critical Mach number; stream Mach number at which $M_l = 1$ is obtained

M_l local Mach number at surface of model

M_f local Mach number in flow field of model

APPARATUS AND TESTS

Tunnel and Model Installations

The tests were conducted in the Langley rectangular high-speed tunnel having a test section 18 inches by 4 inches. The following airfoil sections having 5-inch chords were investigated (fig. 1):

NACA 66,2-015

NACA 66,2-215

Each model completely spanned the test section along the 4-inch dimension and was supported by large circular end plates, fitted so as to rotate as the angle of attack of the model was changed. The juncture between the airfoil and the end plates was sealed and the end plates retained the continuity of surface of the tunnel walls.

One of the circular end plates was fitted with 252 static-pressure orifices each having 0.0135-inch diameter. (See fig. 2.) These orifices were located to permit the measurement of static pressures in a region extending 0.80c above and below the model, 0.20c ahead of the model, and 0.05c behind the model.

Tests and Methods

Airfoil surface pressures near the model semispan and flow-field pressures along the end plate are presented for both models. The cambered airfoil was tested at an angle of attack of 0°, and the symmetrical airfoil was tested at angles of attack of 0° and 6°. The test Mach number extended from approximately 0.30 to the choked tunnel condition. The tunnel choked at a Mach number of approximately 0.80 with a model at an angle of attack of 0° and 0.78 with a model at an angle of attack of 6°. Several different manometer hook-ups were required at each angle of attack to measure the pressure at all the orifices. Because the Mach number changed slightly between hook-ups, it was necessary to plot the experimental pressure values at each orifice against stream Mach number in order to obtain a complete distribution over the flow field at any desired Mach number. By using these faired pressure values and by assuming stream total pressure at all points in the flow, the local Mach numbers in the flow field were computed. Schlieren photographs of the air flow over the symmetrical model were made throughout the Mach number range to supplement the flow-field data. The Reynolds numbers of these tests, which increase with Mach number, range from 700,000 to 1,875,000.

As a supplementary test, the qualitative effect of tunnel-wall boundary layer on the flow-field data was investigated by measuring the chordwise pressure distributions on a $2\frac{1}{2}$-inch-chord NACA 0012 airfoil at various spanwise stations. This model was fitted with two chordwise rows of static-pressure orifices so that the pressure distributions at two spanwise stations could be measured simultaneously. The model had a span of about 10 inches and protruded through the end plates, the junctures being sealed. The model could be moved spanwise across the tunnel so that various spanwise stations could be investigated. Tests were conducted at angles of attack of 0°, 4°, and 6°.

PRECISION

The random errors in the flow-field data should be negligible at almost all Mach numbers because the values presented have been determined from faired data which, in general, vary regularly with Mach number. (See section entitled "Tests and Methods.") The pressures existing at most of the orifices, however, vary rapidly with Mach number at the highest Mach numbers; therefore, at these speeds, the flow-field data are subject to small random errors because of the difficulty in fairing.

Systematic errors resulting from atmospheric humidity, tunnel gradients, calibrations, and air-stream alinement are small.

All local Mach numbers were computed with the assumption of free-stream total pressure. This assumption introduces systematic inaccuracies at all stations inside separated regions or behind shock waves.

The local and stream Mach numbers are subject to error at all test conditions because of tunnel-wall constriction; the error increases as the choking condition is approached. Because adequate constriction corrections to flow conditions in the field of influence of a model have not been devised and because the omission of constriction corrections does not influence the comparisons made in this paper, constriction corrections have not been applied. When a correction to stream Mach number by the method of reference 2 was estimated, it was found that the stream Mach numbers as presented are approximately 0.035 low at a Mach number of 0.790, 0.015 low at 0.700, and 0.002 low at 0.300.

RESULTS AND DISCUSSION

Chordwise Mach Number Distributions

The chordwise Mach number distributions at the tunnel wall along a line 0.1c above the chord line are compared in figure 3 with the surface

chordwise distributions at the midspan location of the NACA 66,2-015 airfoil
at an angle of attack of 0°. At a Mach number of 0.300, the surface velocities
are, as should be expected, slightly higher than those in the field. At
Mach numbers up to 0.750, the pressure recovery characteristics of the model
are such that substream Mach numbers are attained on the surface near the
trailing edge and the field Mach numbers tend to approach stream conditions.
At the highest stream Mach number (near choking), a wide divergence of the
Mach number on the surface and above the surface exists near the trailing
edge.

At an angle of attack of 6° and low Mach numbers (fig. 4), the data
obtained 0.1c above the chord line at the tunnel wall do not indicate the
velocity peaks which are shown by the midspan—surface data. These low
pressure regions near the leading edge of the model may be localized and
extend only a short distance from the model, or the narrow pressure peak
may not be transmitted to the orifice in the tunnel wall because of
relieving effects in the tunnel boundary layer, and thus differences in
flow—field and surface data exist. In other respects, the differences
between the curves are generally not large at or below Mach numbers
of 0.500. At a higher stream Mach number M = 0.700, the surface peak near
the leading edge becomes less pronounced as the velocites over the forward
half of the model surface increase rapidly above the field velocity. As
the Mach number is increased further, the differences between surface and
field conditions over the front half of the model progressively decrease,
whereas the corresponding differences over the rear part of the model
increase rapidly as was the case for the model at an angle of attack of 0°.

As the stream Mach number was increased from 0.700 to 0.775 (fig. 4),
no appreciable change in the local Mach number distribution occurred along
the forward part of the line 0.1c above the chord line. Similar data for
lines 0.2c, 0.4c, and 0.6c above the chord line at an angle of attack
of 6° are presented in figure 5. This figure shows that there is a striking
similarity in the data along the three lines nearest the model. The field
Mach numbers at the 0.6c station above the chord line no longer follow the
trends indicated at the higher speeds and are subsonic throughout for stream
Mach numbers less than 0.700. Furthermore, Mach number contours for this
configuration (fig. 9) show that the supersonic flow region does not approach
the tunnel wall and, therefore, the flow over the upper surface was not
choked at Mach numbers of at least 0.750. The similarity of the data at
various normal—to—chord locations in the flow field appears to be caused by
a fundamental progressive change in type of flow as the stream Mach number is
increased toward unity. At low speeds an appreciable upflow of the air
approaching the leading edge of a lifting airfoil occurs as a result of the
influence of the pressures existing over the whole airfoil surface; in pure
supersonic flows, on the other hand, no influence of the model is felt ahead
of the leading edge. In supercritical flows, the tendency of a local
supersonic region is to maintain the conditions within itself roughly constant

as the stream Mach number increases. These considerations seem to govern
the chordwise variations of local Mach number presented in figures 4 and 5.
Except for the effects of shock-wave movement on the data at the rear part
of the supersonic region the measured local Mach numbers in the supersonic
region of the flow field (and even those foward of the location of $M = 1$)
varied only slightly with stream Mach number. At the surface, however,
where the rate of change of upflow angle with increasing supercritical
Mach numbers is greatest, the local Mach number at forward chordwise
locations decreased appreciably with increase in stream Mach number (within
the Mach number range of fig. 4).

Normal-to-Chord Mach Number Distributions

Figure 6 presents experimental normal-to-chord Mach number gradients
at various chordwise stations for the uncambered airfoil at an angle of
attack of 0°. The surface Mach number at the model semispan has been
plotted as the encircled starting point of the curves. The flow-field
data (measured at the tunnel wall) extend outward from the 10-percent
normal-to-chord station for all chordwise stations between 15 and 75 percent
chord; at the 5- and 85-percent chordwise stations the flow-field data
extend outward from the 5-percent normal-to-chord station. At a Mach
number of 0.300, the induced velocities and the gradients at all chordwise
stations are very small. The practical extent of the model disturbance
appears to be limited to a distance of 1 chord from the model. The surface
points fair smoothly into the flow-field data at this Mach number. At a
Mach number of 0.700, the surface data agree well with the flow-field data.
The gradients, the induced velocities, and the extent of the model
influence are increased above that found at lower Mach numbers. At a Mach
number of 0.775 (fig. 6(c)), the surface data agree well with the flow-
field data at most of the chordwise locations; the effect of flow separation
is apparent, however, in the data for the most rearward chordwise locations
(0.75c and 0.85c). The effect is more noticeable at a Mach number of 0.795
(very near choking) (fig. 6(d)) where the surface velocities are much
higher than those indicated by extrapolation of the flow-field data. At
this Mach number, the curves for the different chordwise stations are not
converging as rapidly as at lower Mach numbers and the extent of the flow
field should therefore be much greater.

Similar effects are noticed in the data for the same airfoil at an
angle of attack of 6°. (See fig. 7.) At this condition the lower-surface
points also agree well with the flow-field data, but the upper-surface
points do not agree as well with the flow field as at an angle of attack
of 0°. Since the surface pressure-distribution measurements at the center
of the tunnel can be well substantiated, the differences between the flow
field and the upper-surface points can be attributed to inaccuracies of the
flow-field measurements. The reaction of the tunnel boundary layer to the
pressure peaks encountered over the upper surface appears to be adversely
affecting the flow-field measurements.

Relieving Effects

The term "relieving effects" as used in this paper implies all effects taking place in the boundary layer which tend to cause the pressure at the tunnel wall to differ from that at a corresponding location in the midspan plane of the model. In order to determine more directly any relieving effects of the tunnel-wall boundary layer, surface pressure distributions were obtained simultaneously at various spanwise stations of an NACA 0012 airfoil. It is believed that the relieving effect at the wall indicated by these surface pressure-distribution measurements at various spanwise stations would be similar to the relieving effect existing along the wall itself.

The results for measuring stations 1/8 inch and 3/8 inch from the tunnel wall (fig. 8) show that the peak pressures obtained 1/8 inch from the wall are appreciably lower than those obtained 3/8 inch from the wall. (Results obtained at the $\frac{3}{8}$-inch station are roughly the same as those obtained at the center line of the tunnel.) The amount of the relieving effect appeared to be a function of the chordwise pressure gradients and the magnitude of the pressure peaks. The presence of the relieving effects discussed in the two preceding sections entitled "Chordwise Mach Number Distributions" and "Normal-to-Chord Mach Number Distributions," is confirmed by these airfoil pressure distributions obtained near the tunnel wall. These results indicate that the flow-field data measured at the wall are reasonably representative of the flow-field conditions at the midspan location for any Mach number except when very steep pressure gradients or flow separation are encountered. When these adverse conditions prevail, the flow-field pressures which find relief through the tunnel-wall boundary layer and the separated region could be more accurately recorded if the tunnel-boundary-layer thickness was reduced. The reduction in boundary-layer thickness might be accomplished by boundary-layer control slots in the tunnel walls or possibly by moving the survey end plate into the air stream in such a manner that the tunnel-boundary-layer air could pass behind it and leave only the undisturbed stream to pass over the survey end plate.

Experimental Flow Field

Experimentally determined contours of constant Mach number in the field of influence of the NACA 66,2-015 airfoil (obtained at the tunnel wall) are presented for the complete test Mach number range in figure 9 at angles of attack of 0° and 6°. The surface pressure data obtained at the midspan of the model were used to determine the Mach number contours near the surface. For comparative purposes, the surface Mach number distributions and the schlieren photographs are also presented for similar test conditions. At a Mach number of 0.300 (fig. 9(a)), good agreement between flow-field and surface-velocity data exists. The schlieren photographs exhibit no density variations at this speed because of the very low induced velocities and smooth flow.

As the Mach number is increased to 0.500 and 0.700 (figs. 9(b) and 9(c), respectively), the velocity—contour spacing decreases very rapidly, especially near the model. At an angle of attack of 6°, the compression shock is first evident at a Mach number of 0.700 (fig. 9(c)); whereas, at an angle of attack of 0°, the shock wave first becomes defined at a Mach number of 0.750 (fig. 9(d)). When the shock wave has grown relatively strong and appreciable separation occurs ($\alpha = 6^{\circ}$, figs. 9(c) and 9(d)), the Mach number contours extend approximately normal from the airfoil in the compression region and thus indicate a reduced velocity gradient normal from the model; probably as a result of the separation, however, the contour lines bend sharply very near the model and approach the surface obliquely. The spacing of the contours decreases rapidly with increasing Mach number in the compression region (figs. 9(a) to 9(d)), but not so rapidly as would be expected from the schlieren photographs; also, the maximum induced velocity indicated by the flow field is somewhat lower than that indicated by the surface velocities. These disagreements appear to result from the combined effects of shock oscillation (reference 3) and pressure relief through the tunnel—wall boundary layer. Consequently, conclusions such as given in reference 4 concerning the position and character of the compression relative to the normal shock wave should not be drawn from these data.

Further increases in Mach number at an angle of attack of 6° (fig. 9(e)) change the character of the shock wave within the field of observation from approximately normal to oblique. A corresponding reduction in the rate of change of the flow—field Mach number with chordwise distance is also shown in the vicinity of the oblique shock. The lower surface undergoes large changes in the maximum local Mach number and in the location of peak velocities at this Mach number.

Comparative contour and pressure—distribution data for the NACA 66,2—215 airfoil (fig. 10) at an angle of attack of 0° show the effect on the flow field of the addition of a slight amount of camber. These data show that the flow field on the upper surface is more extensive for the cambered airfoil than for the symmetrical airfoil at Mach numbers below 0.700. (Compare figs. 9 and 10.) At higher Mach numbers, the airfoil camber becomes increasingly less effective in altering the flow field and, at the highest Mach number (fig. 10(d)), almost no difference exists between the upper-surface and the lower—surface data.

Theoretical Flow Field

The Cauchy contour integral (see appendix and reference 5) was applied to the solution of the velocities or pressures in the flow field of the NACA 66,2—015 airfoil. By this method, the components of total velocity at any point in the flow field of a body at 0° angle of attack are expressed as

$$\frac{u'}{U} = 1 + \frac{1}{2\pi} \oint \left[\left(\frac{u}{U}I - \frac{v}{U}R \right) dx + \left(\frac{u}{U}R + \frac{v}{U}I \right) dy \right]$$

$$\frac{v'}{U} = \frac{1}{2\pi} \oint \left[\left(\frac{u}{U}R + \frac{v}{U}I \right) dx - \left(\frac{u}{U}I - \frac{v}{U}R \right) dy \right]$$

where

$$I = \frac{-(y - y')}{(x - x')^2 + (y - y')^2}$$

$$R = \frac{x - x'}{(x - x')^2 + (y - y')^2}$$

u   component of total velocity in x-direction

U   undisturbed stream velocity

v   component of total velocity in y-direction

x   chordwise station

y   normal-to-chord station

The primed quantities refer to the values in the field, and the unprimed quantities refer to the values on the airfoil surface.

The theoretical pressure distributions of reference 6 were used to obtain the values of surface velocity component u/U and v/U. The solution for the velocity ratios u'/U and v'/U was accomplished by graphical means. Corresponding values of the pressure coefficient were calculated, and contours of constant pressure coefficient were determined.

The calculated contours are compared with experimentally determined contours in figure 11(a). The experimental flow-field data of figure 11 are corrected from $M = 0.300$ to $M = 0$ (incompressible flow) by application of the methods of Ackeret and Prandtl (references 7 and 8 and outlined in reference 9). This correction for compressibility is such that, with increasing stream Mach number above $M = 0$, the distances from the wing

chord for all points on the contour are increased in the ratio $\dfrac{1}{\sqrt{1 - M^2}}$

and the corresponding value of the pressure coefficient is increased in the same ratio. Although it appears that some effects of pressure relief are present in these data, reasonably good agreement between theory and experiment has been obtained for incompressible flow. In view of this agreement, it appears that low—speed experimental rather than theoretical surface—velocity components could be used with equally good results in the theoretical computation of the flow field.

Variation of Flow—Field Mach Number with Stream Mach Number

The variations with stream Mach number of the Mach numbers on the air-foil surface (obtained at the midspan of the model) and at several represen-tative locations in the field of the model (obtained at the tunnel wall) are presented in figure 12. Corresponding theoretical variations (references 9 to 11) are also included. At the 5—percent chordwise station the estimated flow—field data differ appreciably from the measured data at both angles of attack. At an angle of attack of 0° (fig. 12(a)), however, the agreement of theory and experiment at the 5—percent chordwise station becomes much improved as the normal—to—chord distance from the model increases. At all other conditions shown in figure 12, the experimental and theoretical variations of flow—field Mach number with stream Mach number are in close agreement at Mach numbers up to 0.700.

Therefore, by the application of methods of Ackeret and Prandtl (references 7 to 9), velocity conditions at subcritical Mach numbers in the field of bodies may be estimated very accurately from low—speed tunnel data. In some cases the estimation can be applied at Mach numbers in excess of the critical.

Practical Considerations

The experimental low—speed flow—field contours (corrected to $M = 0$) have been shown to be in agreement with those computed by means of the Cauchy contour integral. Furthermore, the low—speed flow—field data of this paper were extrapolated by the application of the methods of Ackeret and Prandtl to provide accurate flow—field data at higher Mach numbers. Therefore, it might be expected that the flow field about an airfoil could be determined with adequate accuracy for practical purposes at any subcritical Mach number if only its theoretical or experimental surface pressure distribution is known.

CONCLUSIONS

An investigation of the two-dimensional flow-field conditions near
an airfoil surface, conducted by measuring the static pressures existing
along the end plate of the model, has indicated the following conclusions:

1. Reasonably good agreement was obtained between the experimental flow-
field pressure contours (corrected to the stream Mach number M = 0
from M = 0.300) and those determined theoretically for incompressible flow
by means of the Cauchy contour integral.

2. Low-speed flow-field data can be extended for use at subcritical
Mach numbers by the application of the methods of Prandtl and Ackeret.

3. The flow-field pressures measured at the wall, when judged by their
relation to the midspan surface pressures, appeared to be reasonably
representative of conditions at the midspan location in the field, except
when steep pressure gradients or flow separation were encountered.

Langley Aeronautical Laboratory
       National Advisory Committee for Aeronautics
              Langley Air Force Base, Va., December 31, 1948

APPENDIX

METHOD OF APPLICATION OF THE CAUCHY CONTOUR INTEGRAL

The method whereby the Cauchy contour integral was applied to obtain the velocity distribution in the field of the NACA 66,2-015 airfoil is as follows:

If W is the complex potential function

$$W = \emptyset + i\psi$$

where

$\emptyset$ velocity potential

ψ stream function

$i = \sqrt{-1}$

and if

$$Z = x + iy$$

then

$$\frac{dW}{dZ} = u - iv \qquad\qquad (1)$$

where

u   component of total velocity in x-direction

v   component of total velocity in y-direction

x   chordwise location

y   normal-to-chord location

By the Cauchy integral formula applied to residues (reference 5)

$$\frac{1}{2\pi i} \oint_{c} f(Z)dZ = (K' + K'' + \ldots + K^n) \tag{2}$$

where $f(Z)$ is analytic within and on a closed curve c except at a finite number of singular points Z', Z'', $\ldots Z^n$ having residues which are K', K'', $\ldots K^n$, respectively.

If the path of integration is taken about the simply connected region r
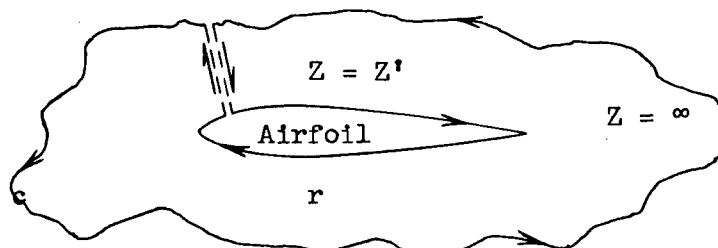
(extending to infinity) containing singular points at $Z = Z'$ and $Z = \infty$, then

$$\frac{1}{2\pi i} \oint_{c} \frac{\frac{dW}{dZ}}{Z - Z'} dZ = \left(K_{Z=Z'} + K_{Z=\infty}\right) \tag{3}$$

where Z' is the field point (x',y') at which the velocities are required. Also

$$K_{Z=\infty} = -\left(\frac{dW}{dZ}\right)_{Z=\infty} = -U(\cos \alpha + i \sin \alpha)$$

and

$$K_{Z=Z'} = \left(\frac{dW}{dZ}\right)_{Z=Z'} = \frac{1}{2\pi i} \oint_{c} \left[(u - iv)(R + iI)(dx + i\, dy)\right]$$

$$+ U(\cos \alpha + i \sin \alpha) \tag{4}$$

where

R   real part of $\dfrac{1}{Z - Z'}$

I   imaginary part of $\dfrac{1}{Z - Z'}$

U   stream velocity

α   angle of attack

Then, where primed quantities refer to the point in the field and the unprimed quantities refer to the airfoil surface

$$R + iI = \frac{1}{(x + iy) - (x' + iy')} = \frac{(x - x') - i(y - y')}{(x - x')^2 + (y - y')^2}$$

and, therefore,

$$R = \frac{x - x'}{(x - x')^2 + (y - y')^2} \tag{5}$$

$$I = \frac{-(y - y')}{(x - x')^2 + (y - y')^2} \tag{6}$$

From equation (4)

$$u' - iv' = U(\cos\alpha + i\sin\alpha) + \frac{1}{2\pi i} \oint \left[(uR + vI - ivR + iuI)(dx + i\,dy)\right]$$

$$= U(\cos\alpha + i\sin\alpha) + \frac{1}{2\pi i} \oint \left[(uR + vI)dx + (vR - uI)dy - i(vR - uI)dx\right.$$

$$\left. + i(uR + vI)dy\right] \tag{7}$$

but u' equals the real part of the right—hand side of equation (7), and iv' equals the imaginary part of the right—hand side of equation (7); therefore,

$$u' = U(\cos\alpha) + \frac{1}{2\pi}\oint\left[(uI - vR)dx + (uR + vI)dy\right] \qquad (8)$$

$$v' = U\sin\alpha + \frac{1}{2\pi}\oint\left[(uR + vI)dx - (uI - vR)dy\right] \qquad (9)$$

or nondimensionally

$$\frac{u'}{U} = \cos\alpha + \frac{1}{2\pi}\oint\left[\left(\frac{u}{U}I - \frac{v}{U}R\right)dx + \left(\frac{u}{U}R + \frac{v}{U}I\right)dy\right] \qquad (10)$$

$$\frac{v'}{U} = \sin\alpha + \frac{1}{2\pi}\oint\left[\left(\frac{u}{U}R + \frac{v}{U}I\right)dx - \left(\frac{u}{U}I - \frac{v}{U}R\right)dy\right] \qquad (11)$$

The velocity ratios at the airfoil surface u/U and v/U, and the values of R and I (equations (5) and (6)) therefore determine the velocity ratios in the flow field u'/U and v'/U when the integral is taken about the simply connected region. The solution of equations (10) and (11) was accomplished by graphical means.

When these values of the flow-field velocity ratio are used, the pressure coefficient at the corresponding point (x',y') in the flow field is defined as

$$P = 1 - \left[\left(\frac{v'}{U}\right)^2 + \left(\frac{u'}{U}\right)^2\right] \qquad (12)$$

The values of the surface-velocity components u/U and v/U were obtained from the theoretical data on basic thickness forms given in reference 6.

REFERENCES

1. Ackeret, J., Feldman, F., and Rott, N.: Investigations of Compression Shocks and Boundary Layers in Gases Moving at High Speed. NACA TM No. 1113, 1947.

2. Allen, H. Julian, and Vincenti, Walter G.: The Wall Interference in a Two-Dimensional-Flow Wind Tunnel with Consideration of the Effect of Compressibility. NACA Rep. No. 782, 1944.

3. Daley, Bernard N., and Humphreys, Milton D.: Effects of Compressibility on the Flow past Thick Airfoil Sections. NACA TN No. 1657, 1948.

4. Donaldson, Coleman duP.: Effects of Interaction between Normal Shock and Boundary Layer. NACA CB No. 4A27, 1944.

5. Whittaker, E. T., and Watson, G. N.: A Course of Modern Analysis. Fourth ed., Cambridge Univ. Press (London), 1927, p. 119.

6. Abbott, Ira H., Von Doenhoff, Albert E., and Stivers, Louis S., Jr.: Summary of Airfoil Data. NACA Rep. No. 824, 1945.

7. Ackeret, J.: Über Luftkräfte bei sehr grossen Geschwindigkeiten insbesondere bei ebenen Strömungen. Helvetica Physica Acta, vol. 1, fasc. 5, 1928, pp. 301-322.

8. Prandtl, L.: General Considerations on the Flow of Compressible Fluids. NACA TM No. 805, 1936.

9. Delano, James B., and Wright, Ray H.: Investigation of Drag and Pressure Distribution of Windshields at High Speeds. NACA ARR, Jan. 1942.

10. Glauert, H.: The Effect of Compressibility on the Lift of an Aerofoil. R. & M. No. 1135, British A.R.C., 1927.

11. Kaplan, Carl: The Flow of a Compressible Fluid past a Curved Surface. NACA Rep. No. 768, 1943.
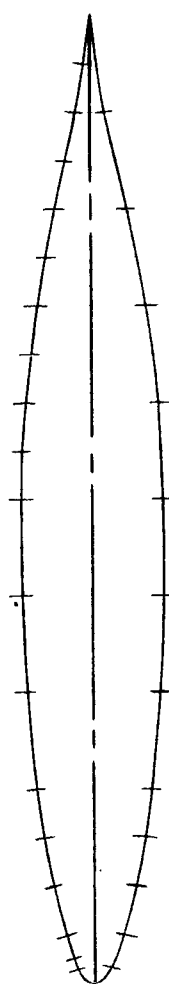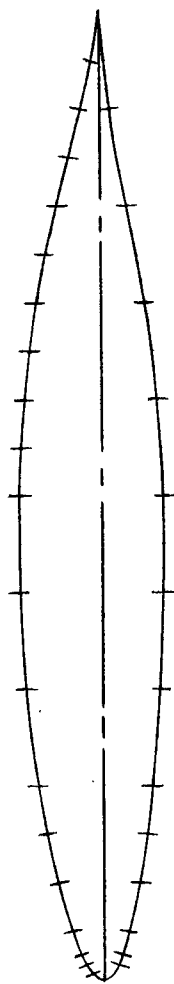
Figure 1.— Airfoil profiles and static-pressure-orifice locations.
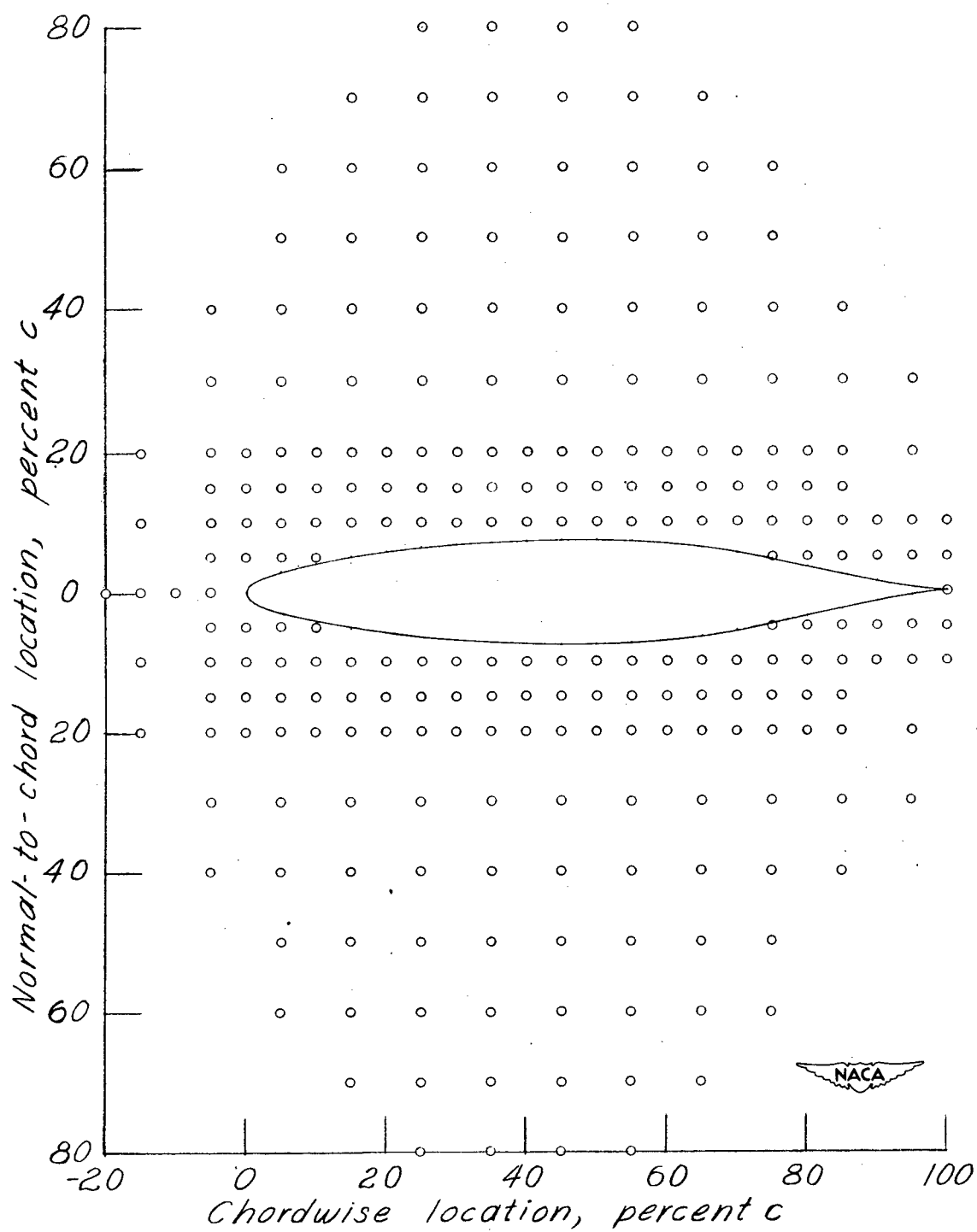
Figure 2.- Locations of pressure orifices in survey end plate relative to the NACA 66,2-015 airfoil.
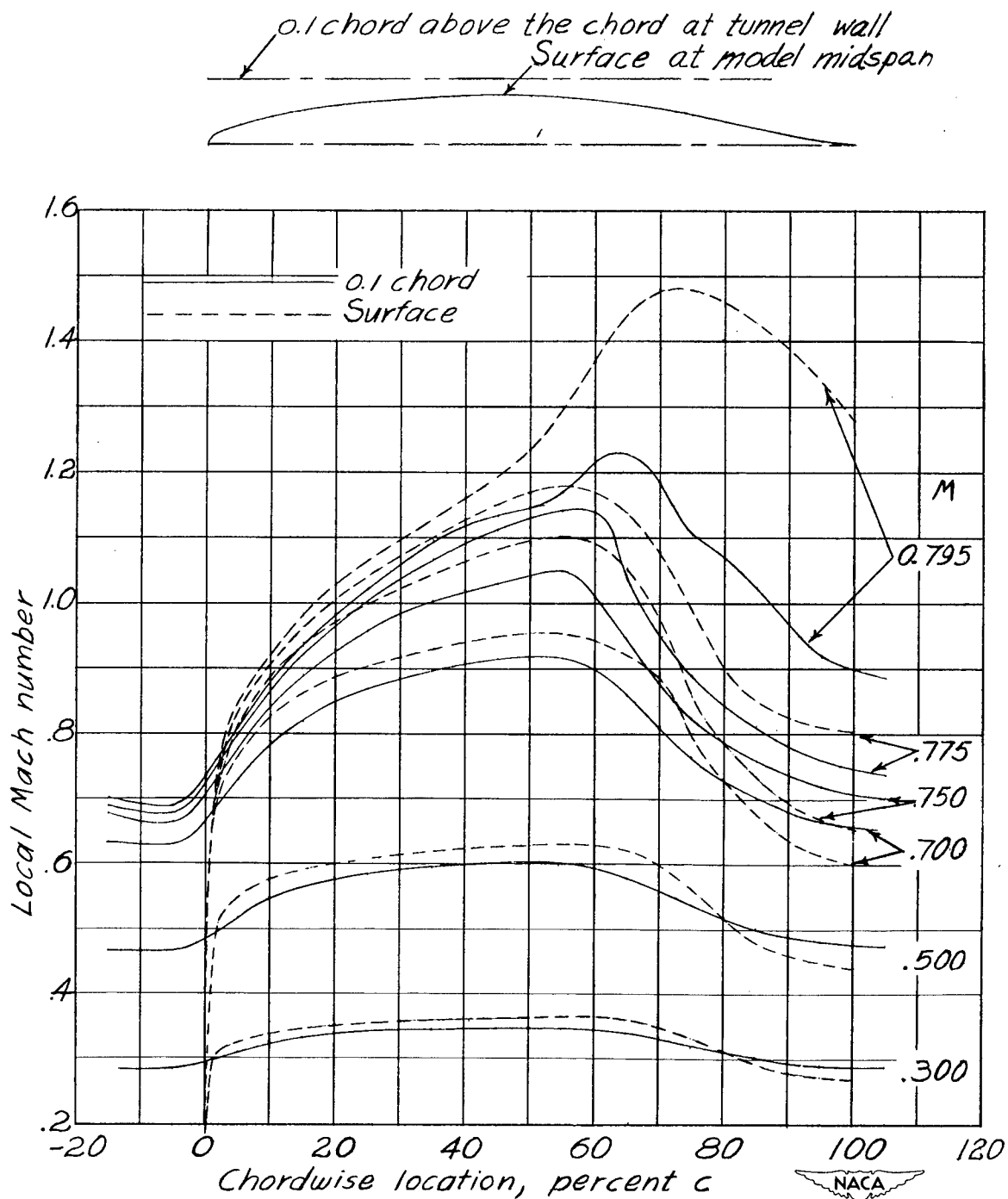
Figure 3.— Mach number distributions along the surface and along a line 0.1 chord above the chord line of the NACA 66,2 - 015 airfoil. $\alpha = 0°$
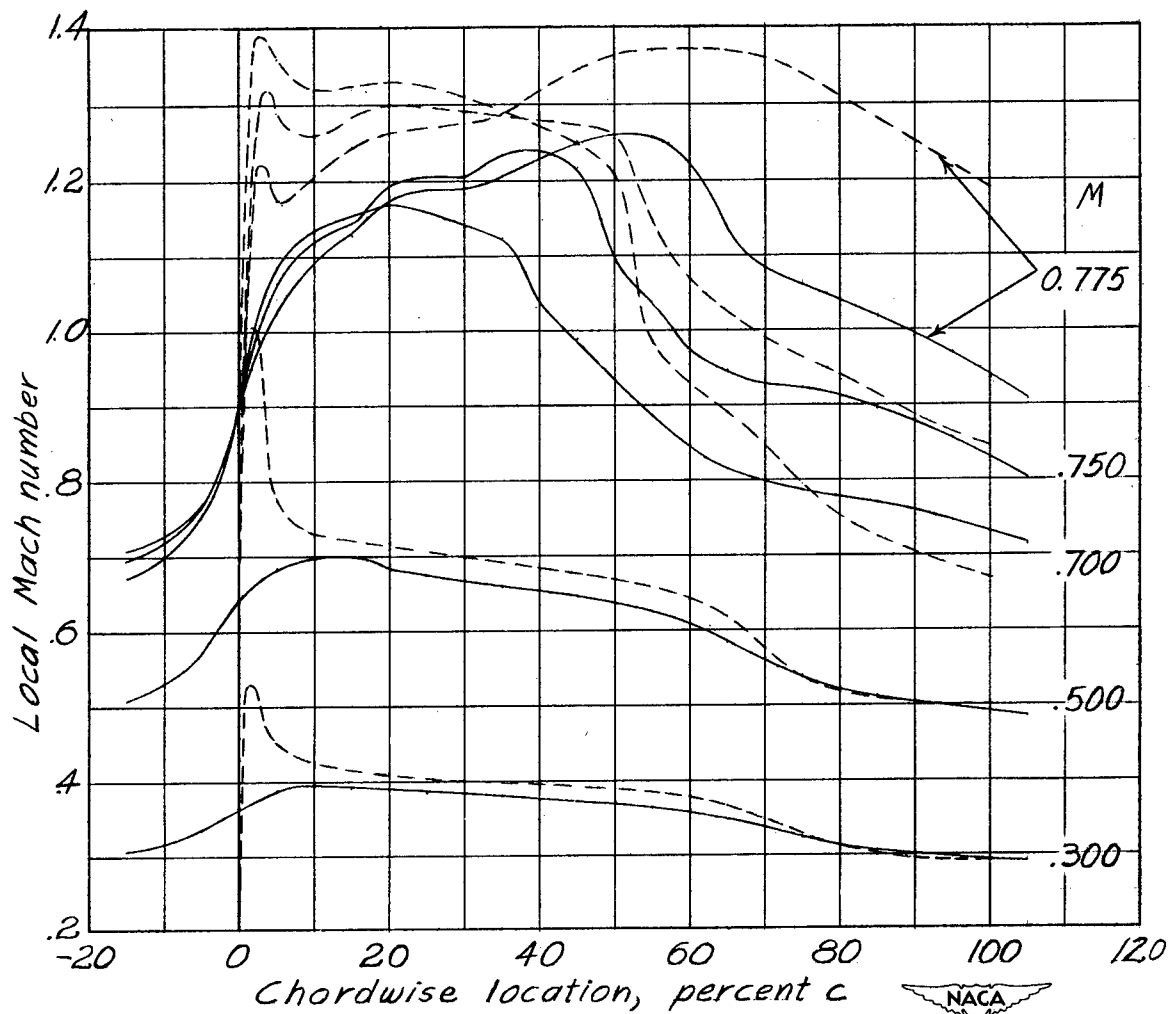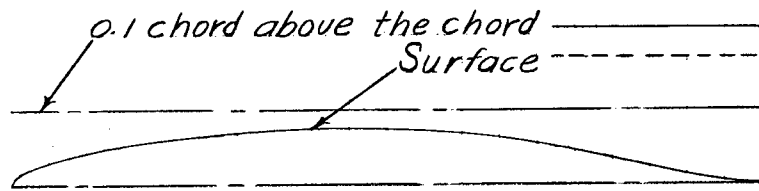
Figure 4.— Mach number distributions along the surface and along a line 0.1 chord above the chord line of the NACA 66,2-015 airfoil. $\alpha = 6°$.
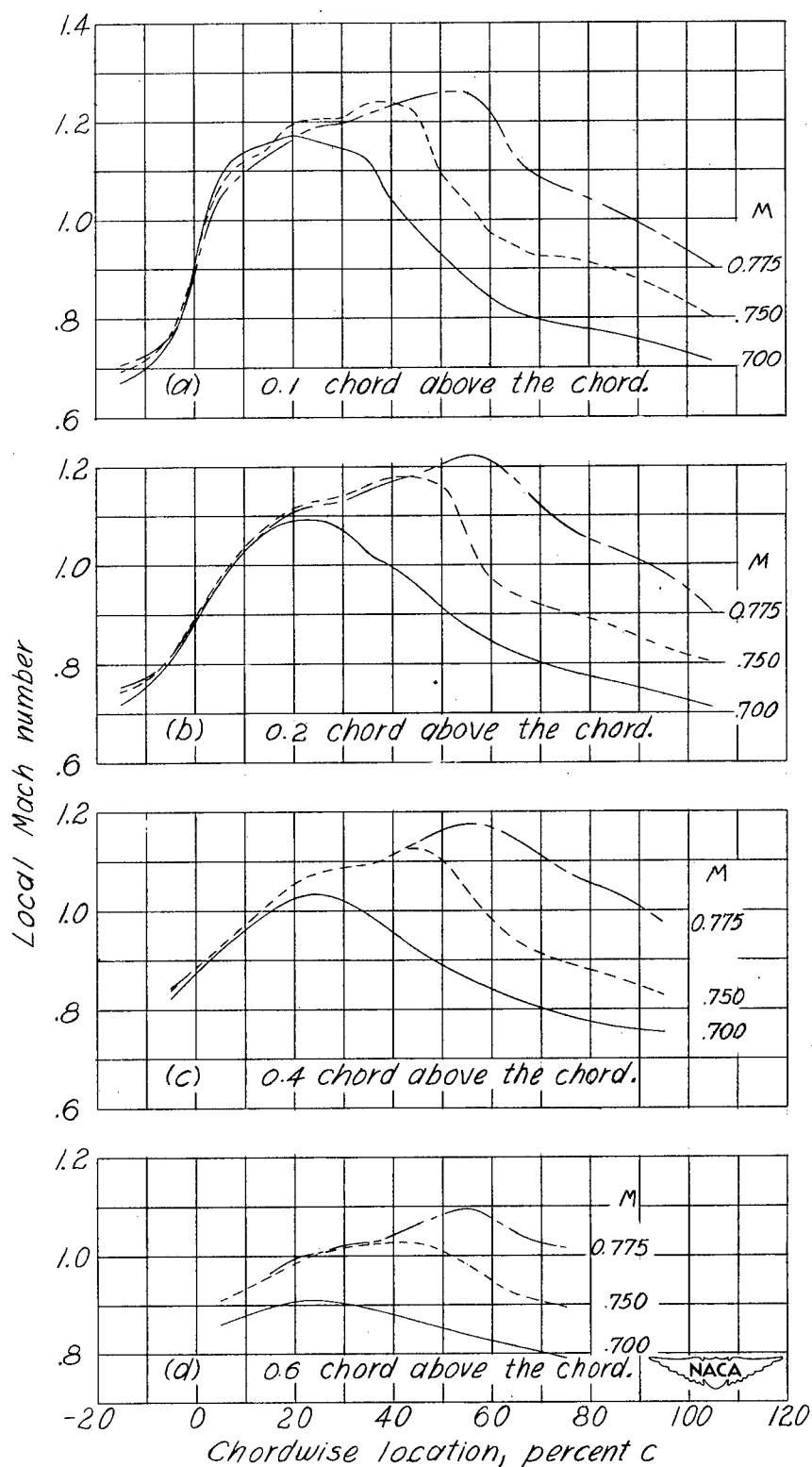
Figure 5.— A comparison of the chordwise distributions of the local Mach number at several locations in the flow field; NACA 66,2-015 airfoil; $\alpha = 6°$.

(a)   M = 0.300.
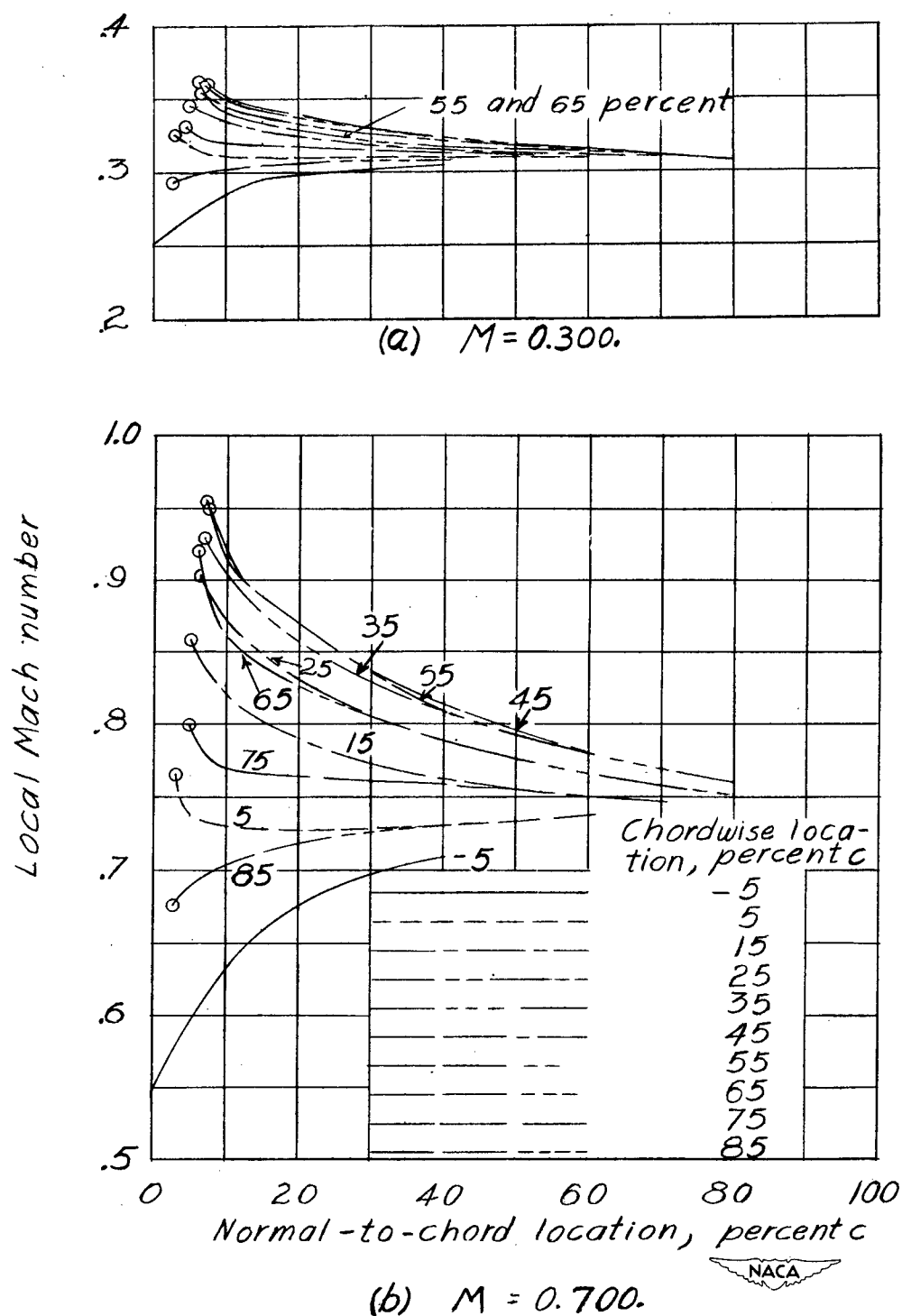
(b)   M = 0.700.

Figure 6.— Variation of local Mach number along lines perpendicular to chord and at various distances from leading edge. NACA 66,2-015; α=0°
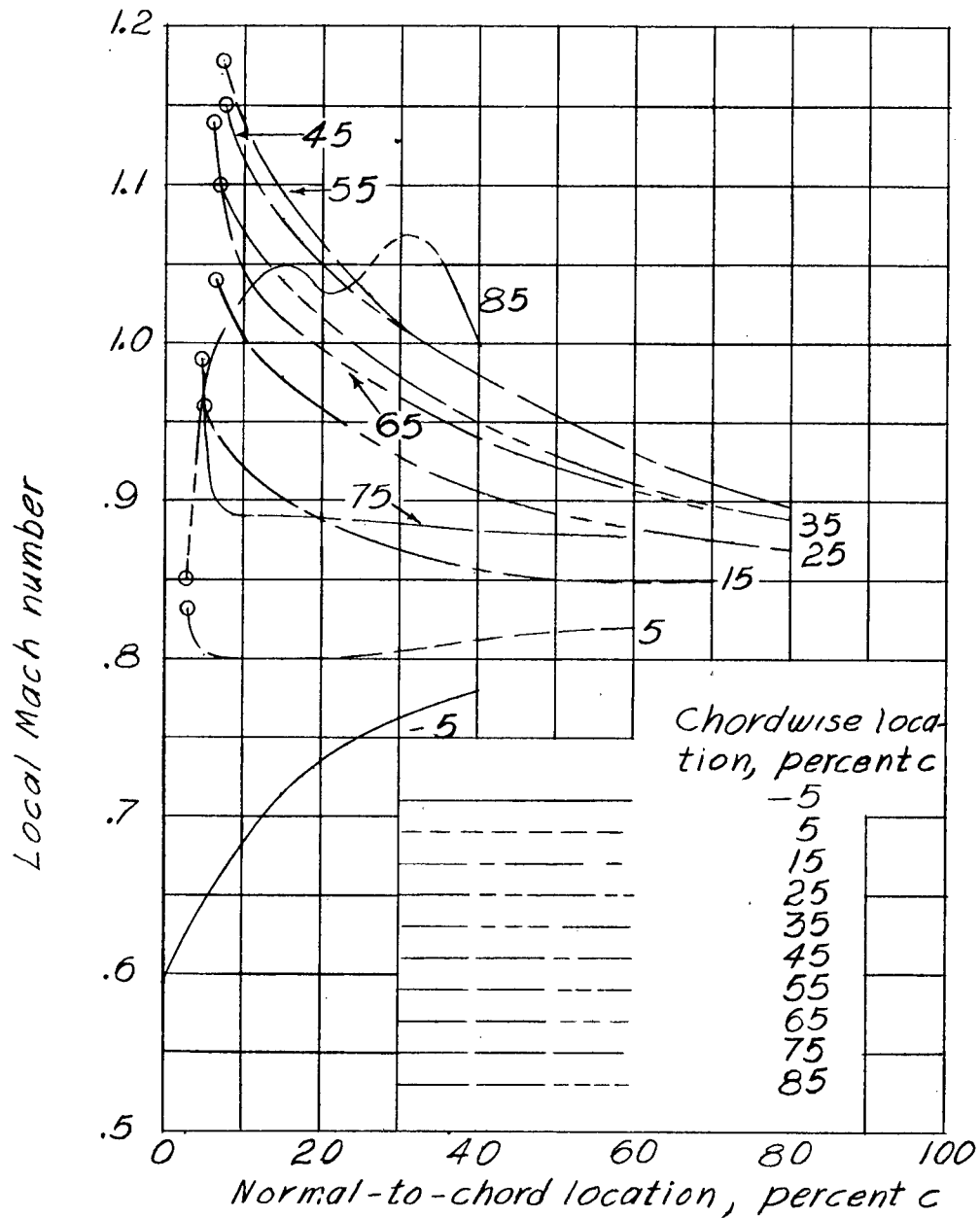
(c) M = 0.775.

Figure 6.— Continued.

(d)   M = 0.795.
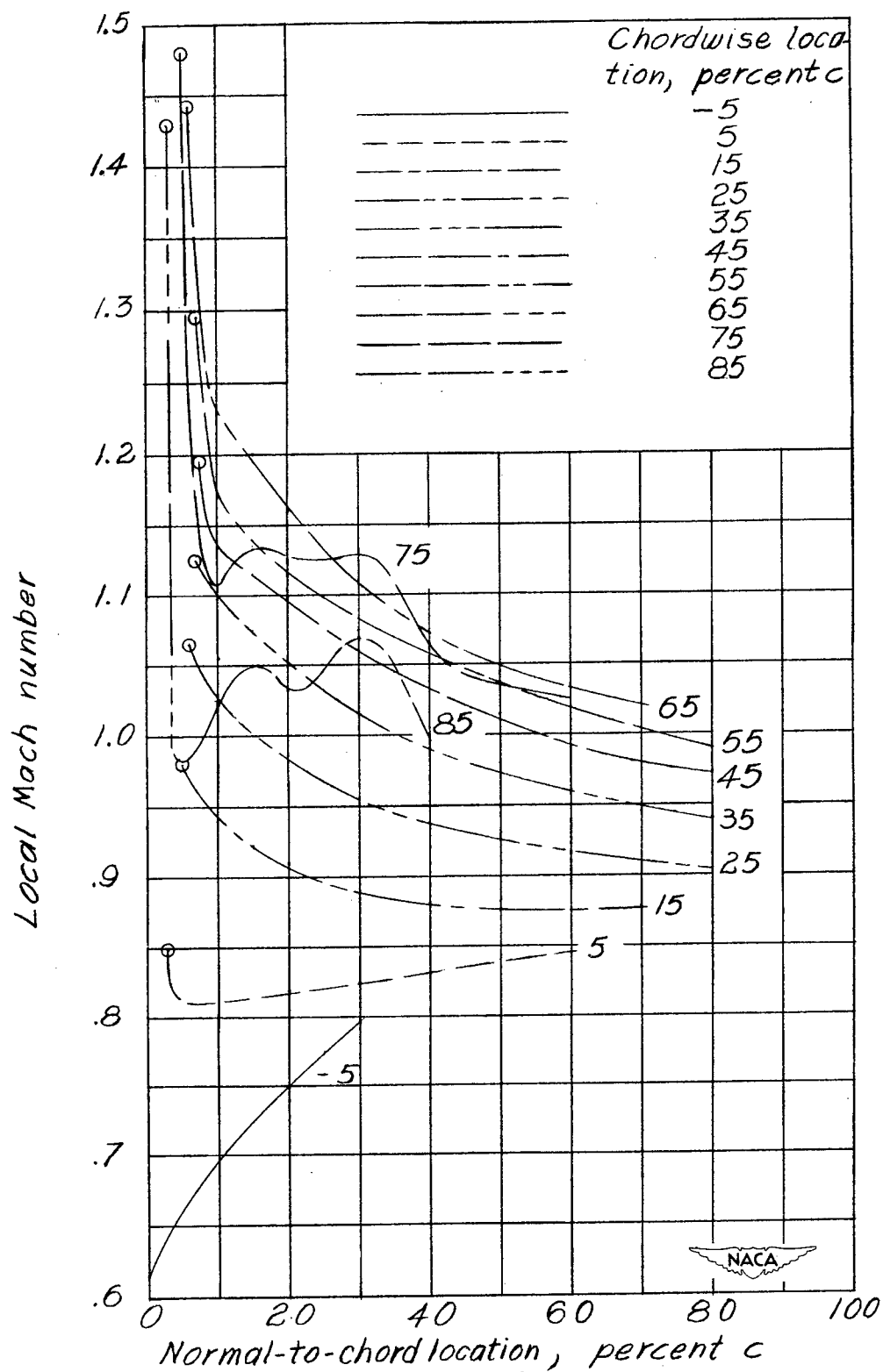
Figure 6.— Concluded.
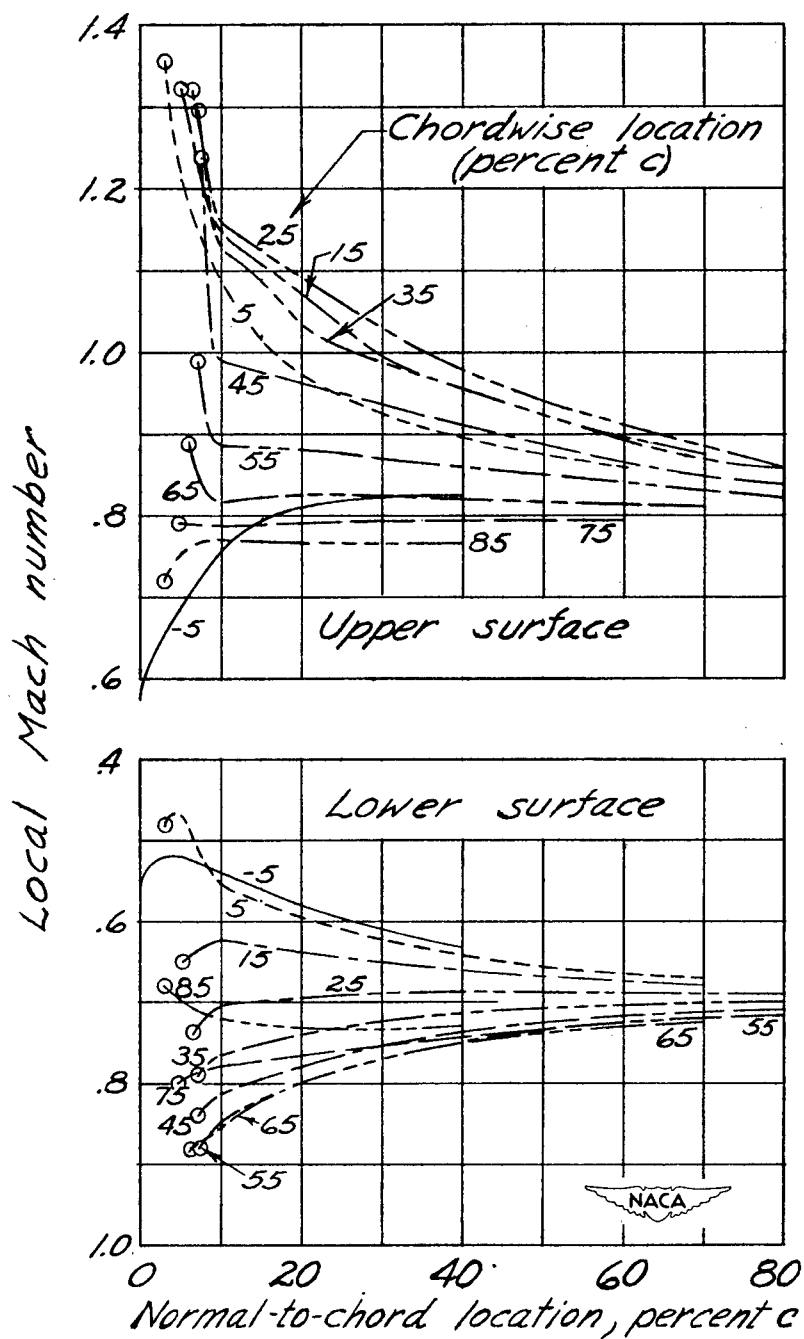
(a) M = 0.700.

Figure 7.— Variation of local Mach number along lines perpendicular to the chord at various distances from the leading edge. NACA 66,2-015 airfoil; α = 6°.
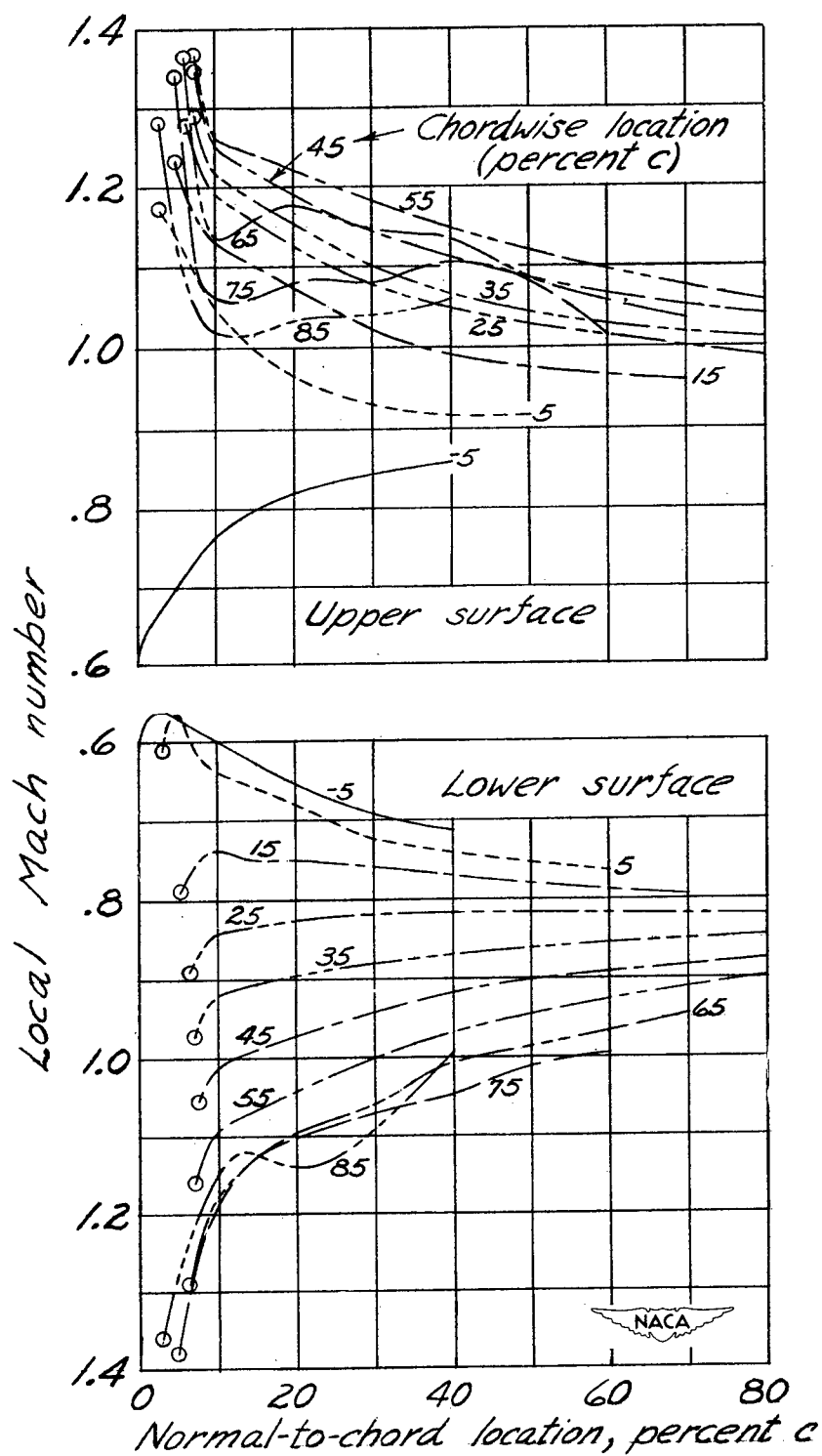
(b) M=0.775.

Figure 7.—Concluded.
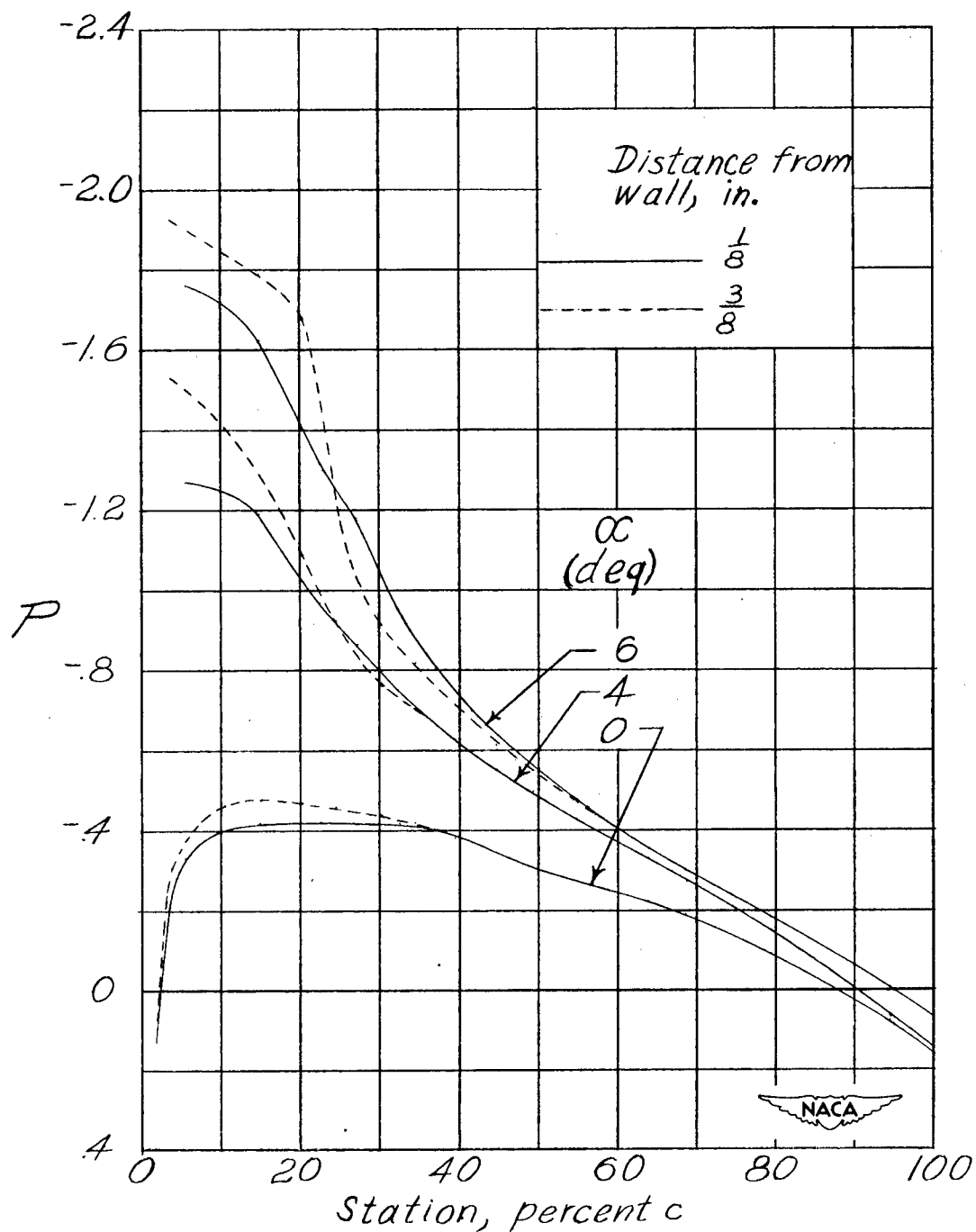
Figure 8.— Comparison of pressure distributions obtained at various spanwise distances from the wall of the Langley rectangular high-speed tunnel. Upper surface of NACA 0012 airfoil, M=0.650.
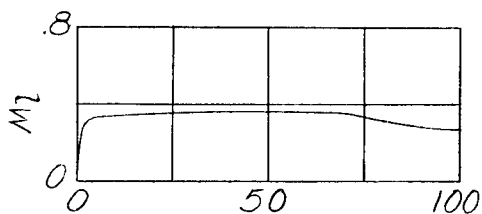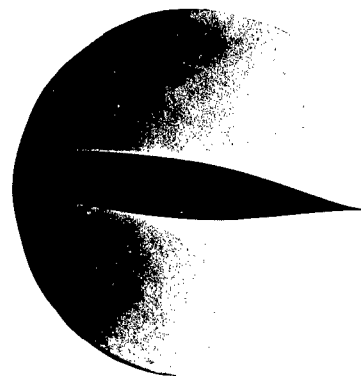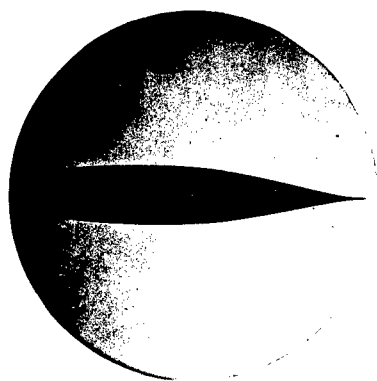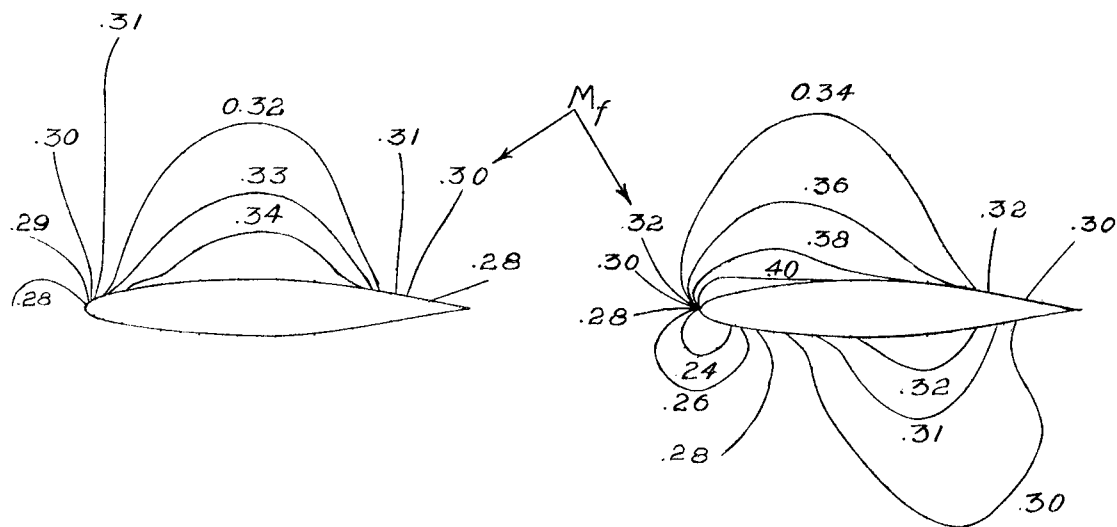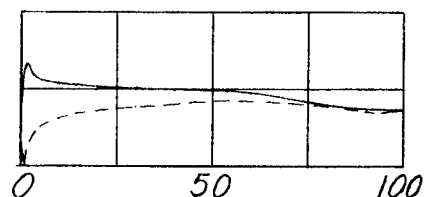
(a) $M = 0.300$.

Figure 9.— Details of flow phenomena. NACA 66,2-015 airfoil.
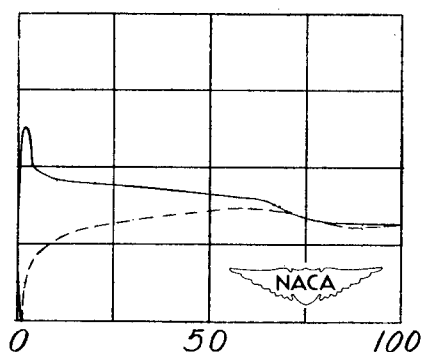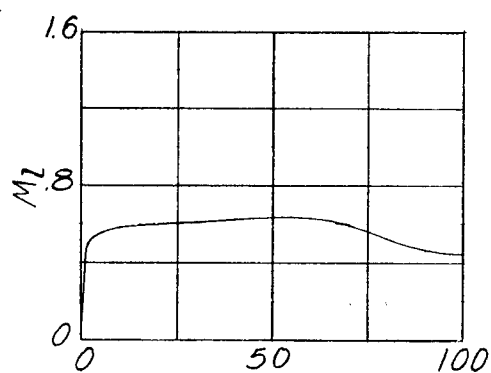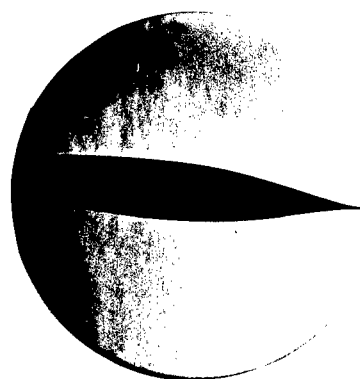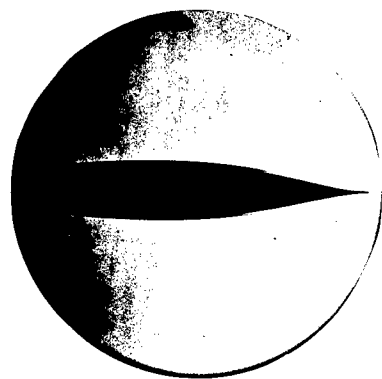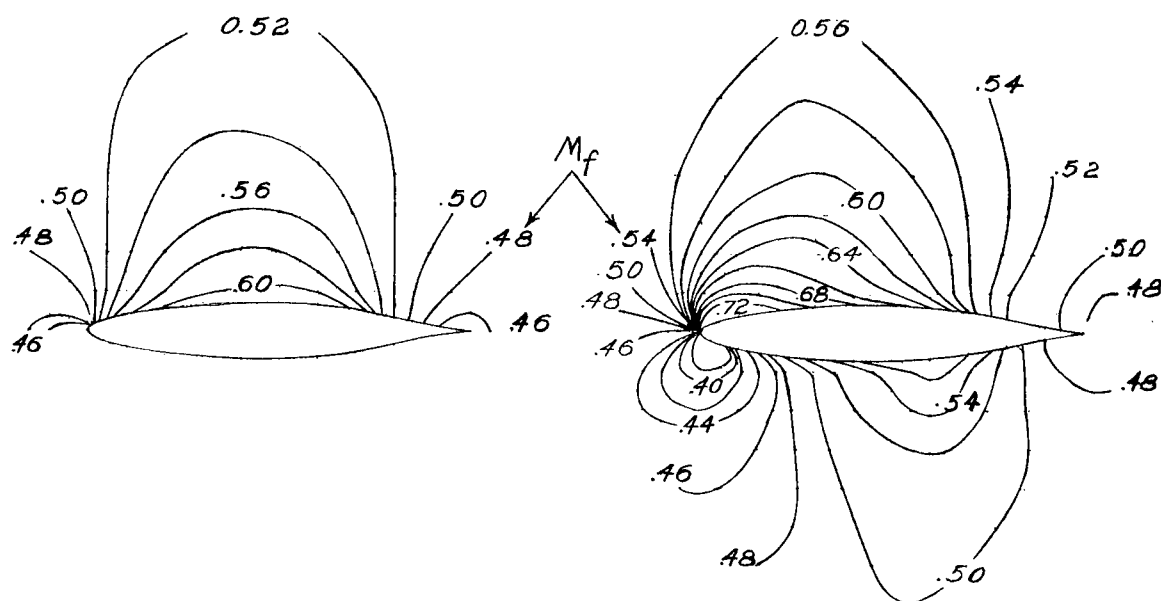
(b) M = 0.500.

figure 9.— Continued.

M_f

M_L

$\alpha = 0°$

Station, percent c

$\alpha = 6°$
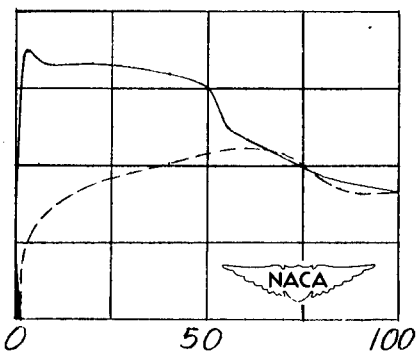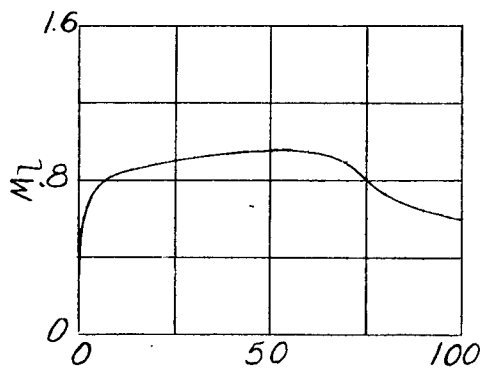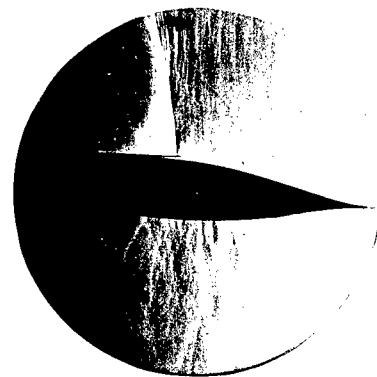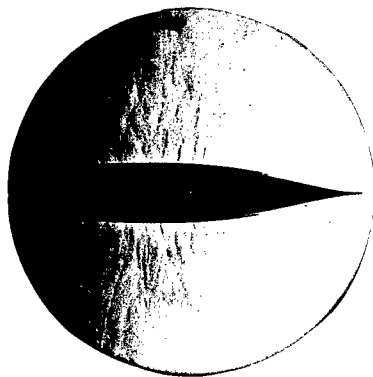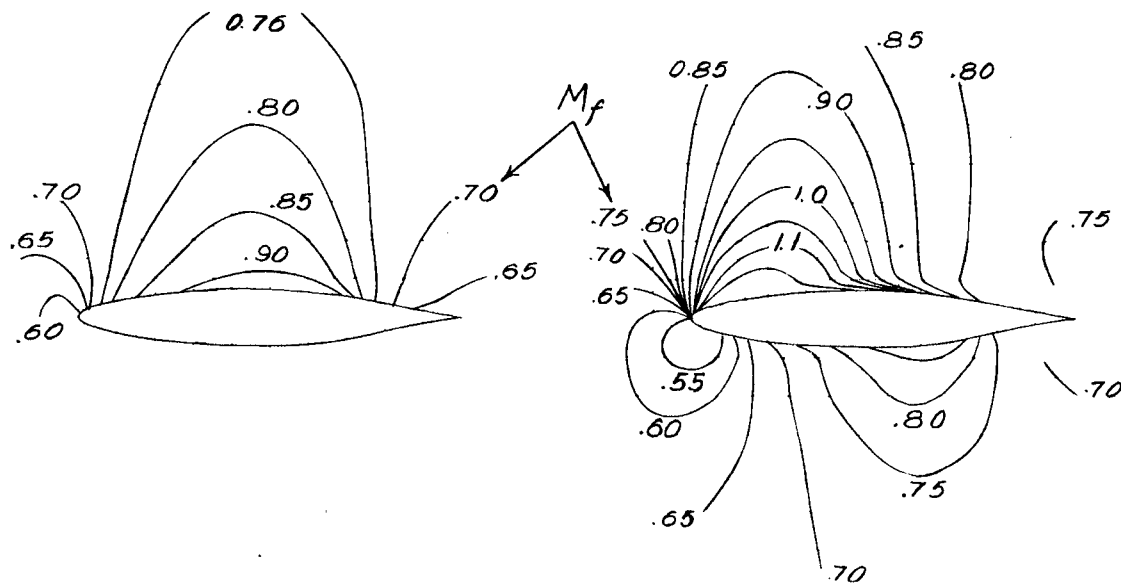
(c) M = 0.700.
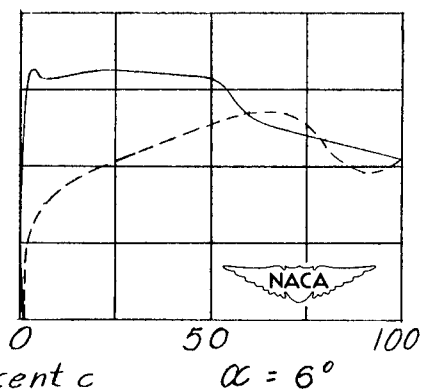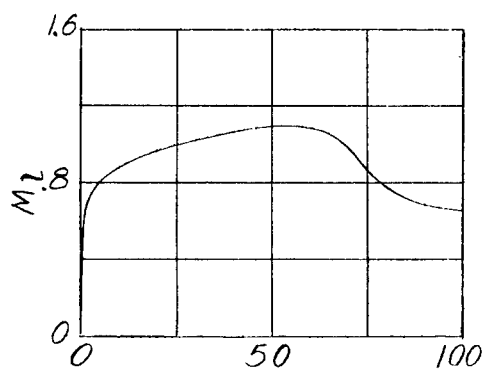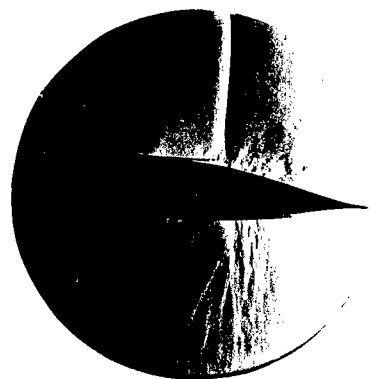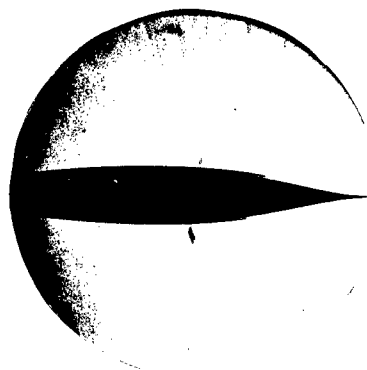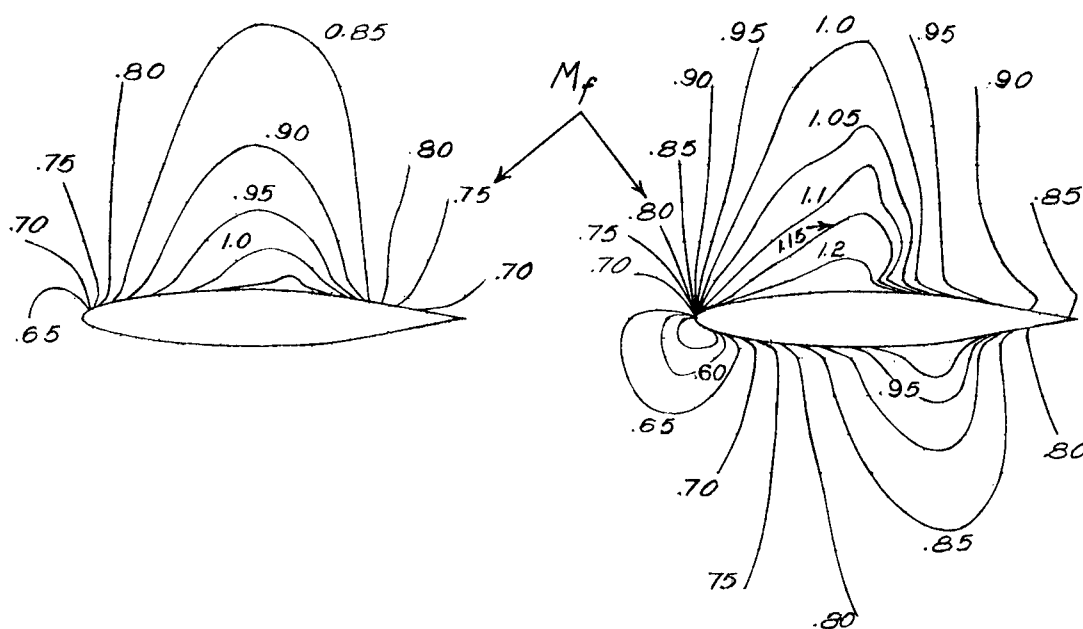
Figure 9.— Continued.

(d) M = 0.750.
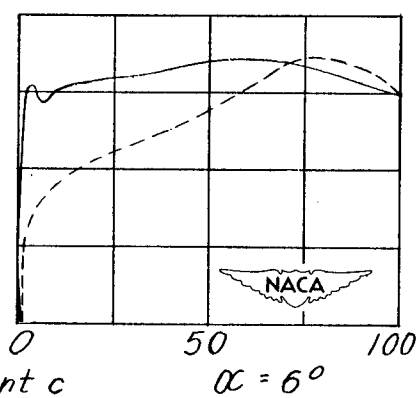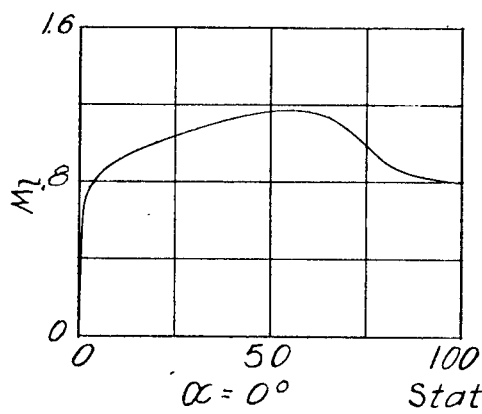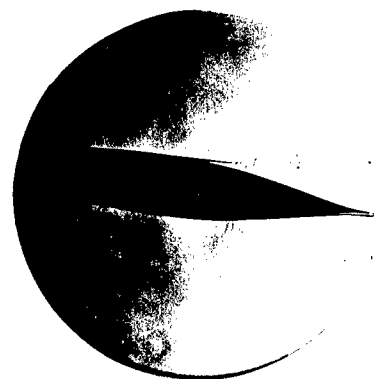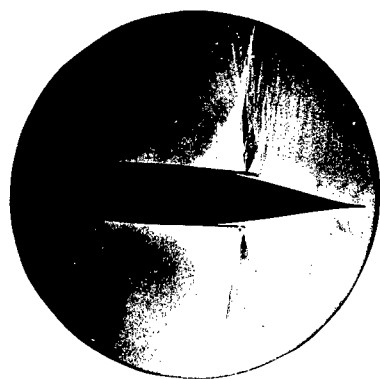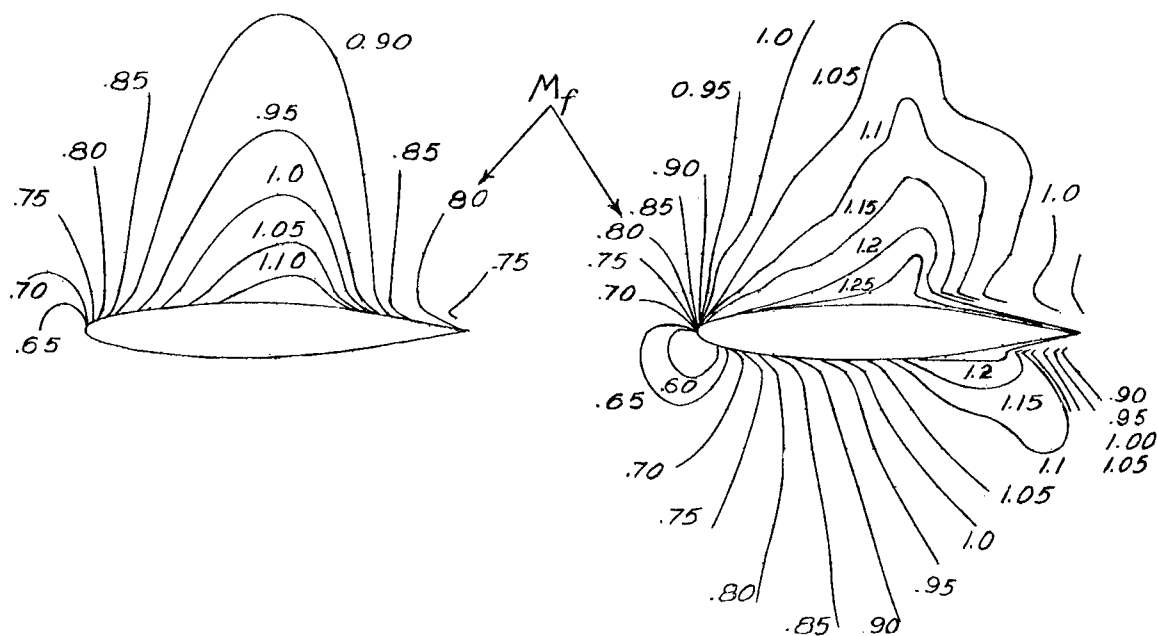
Figure 9.— Continued.

(e) M = 0.775.

Figure 9.— Continued.

Station, percent c

$\alpha = 0°$

(f) = M = 0.795.
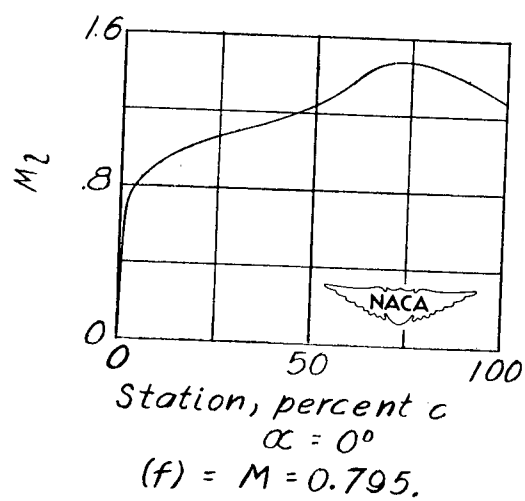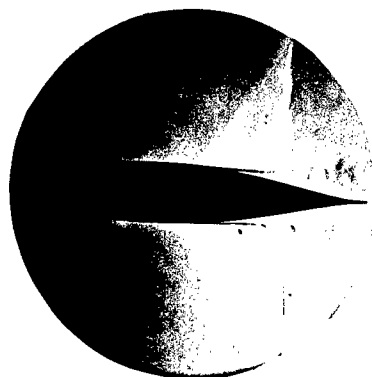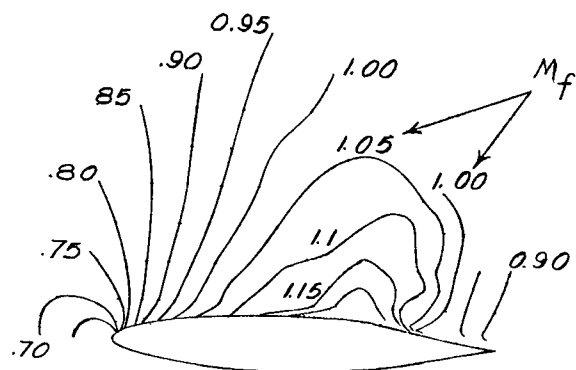
Figure 9.— Concluded.

M_f
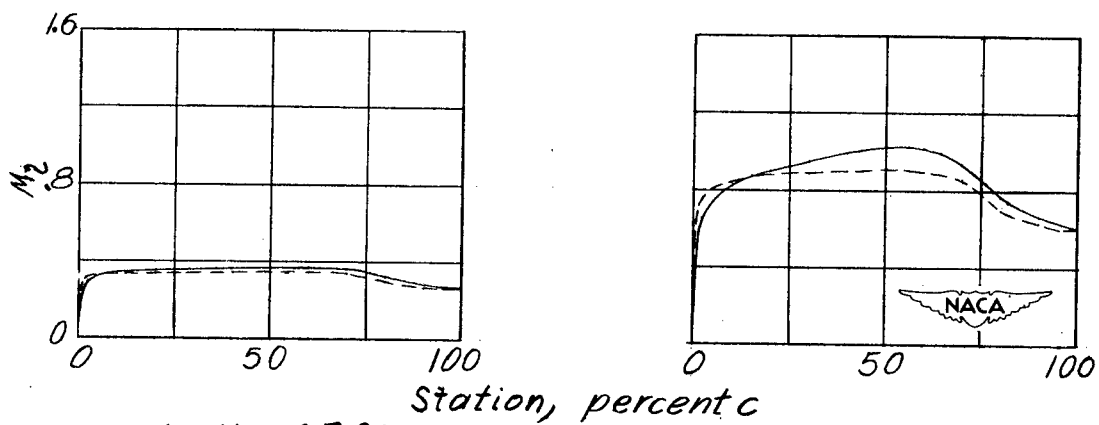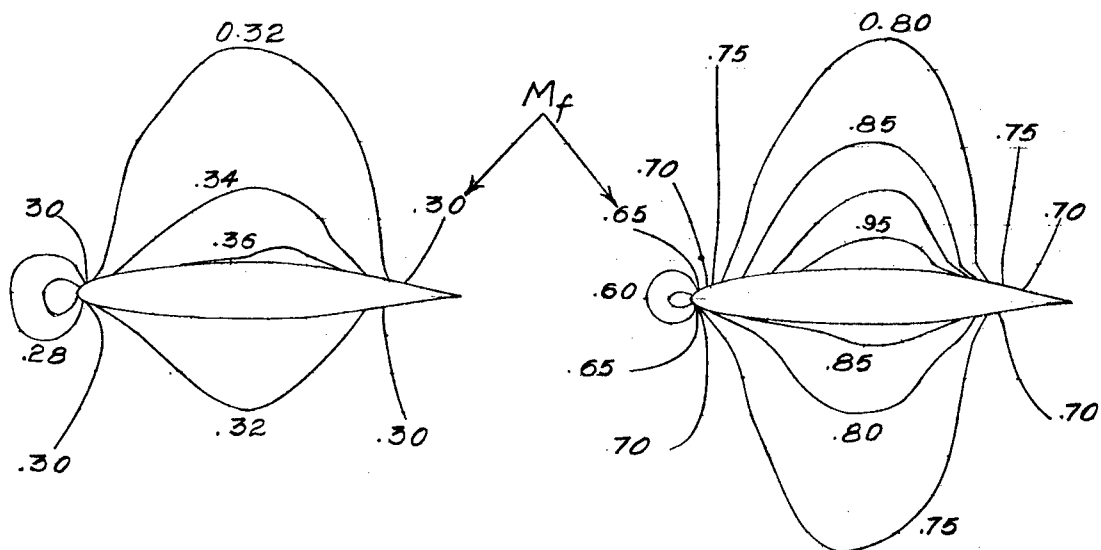
(a) M = 0.300.   (b) M = 0.700.

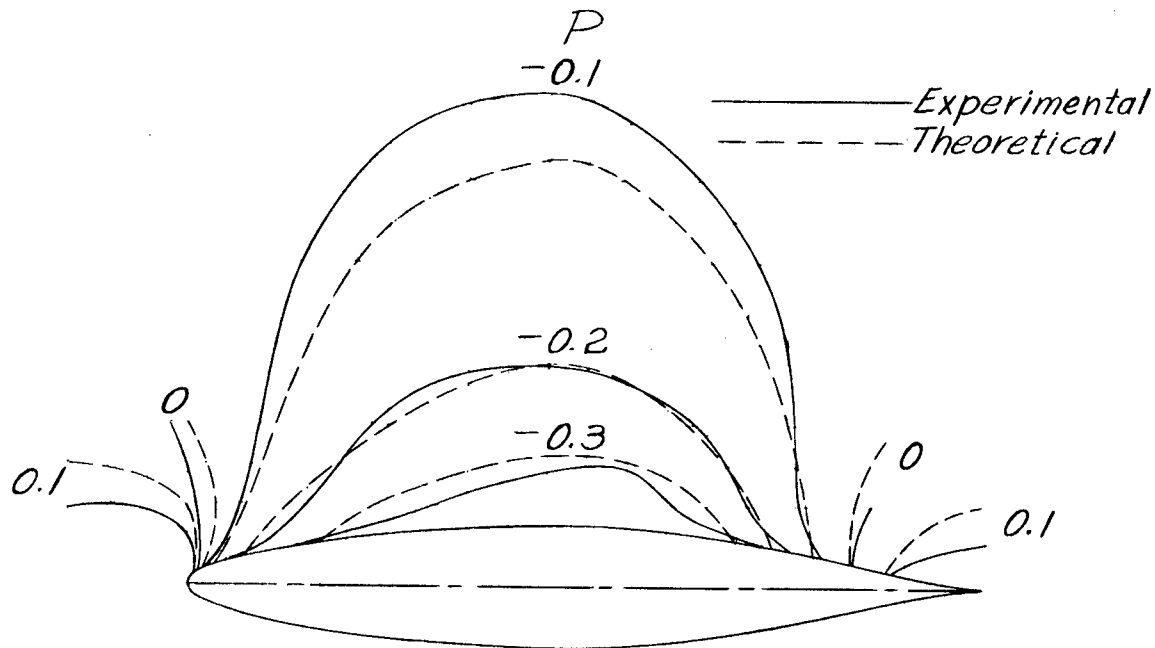Figure 10.— Details of flow phenomenon. NACA 66,2-215 airfoil; α = 0°.
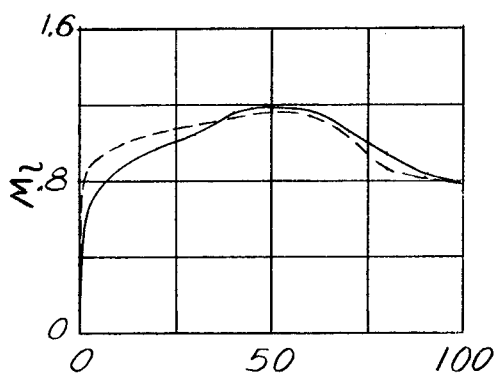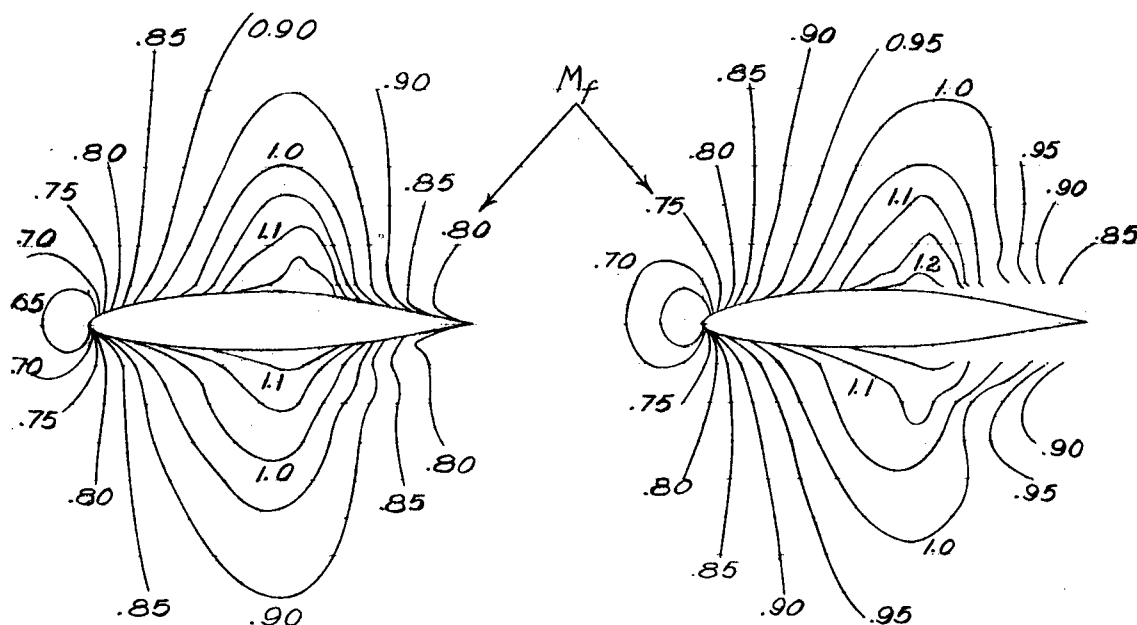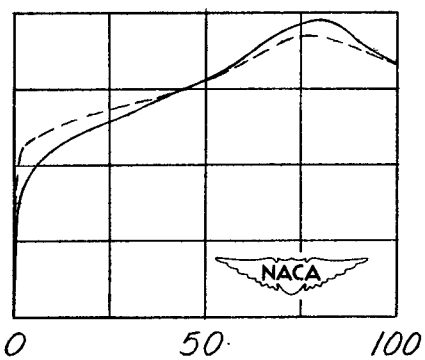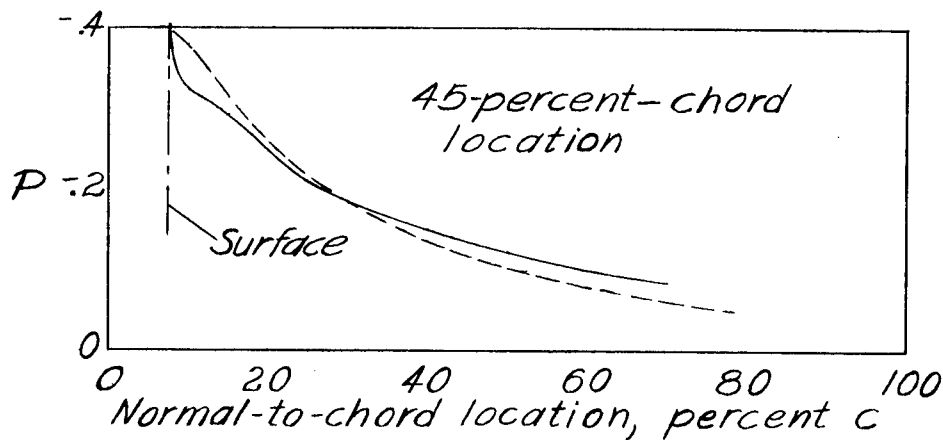
(c) M = 0.775.   (d) M = 0.790.
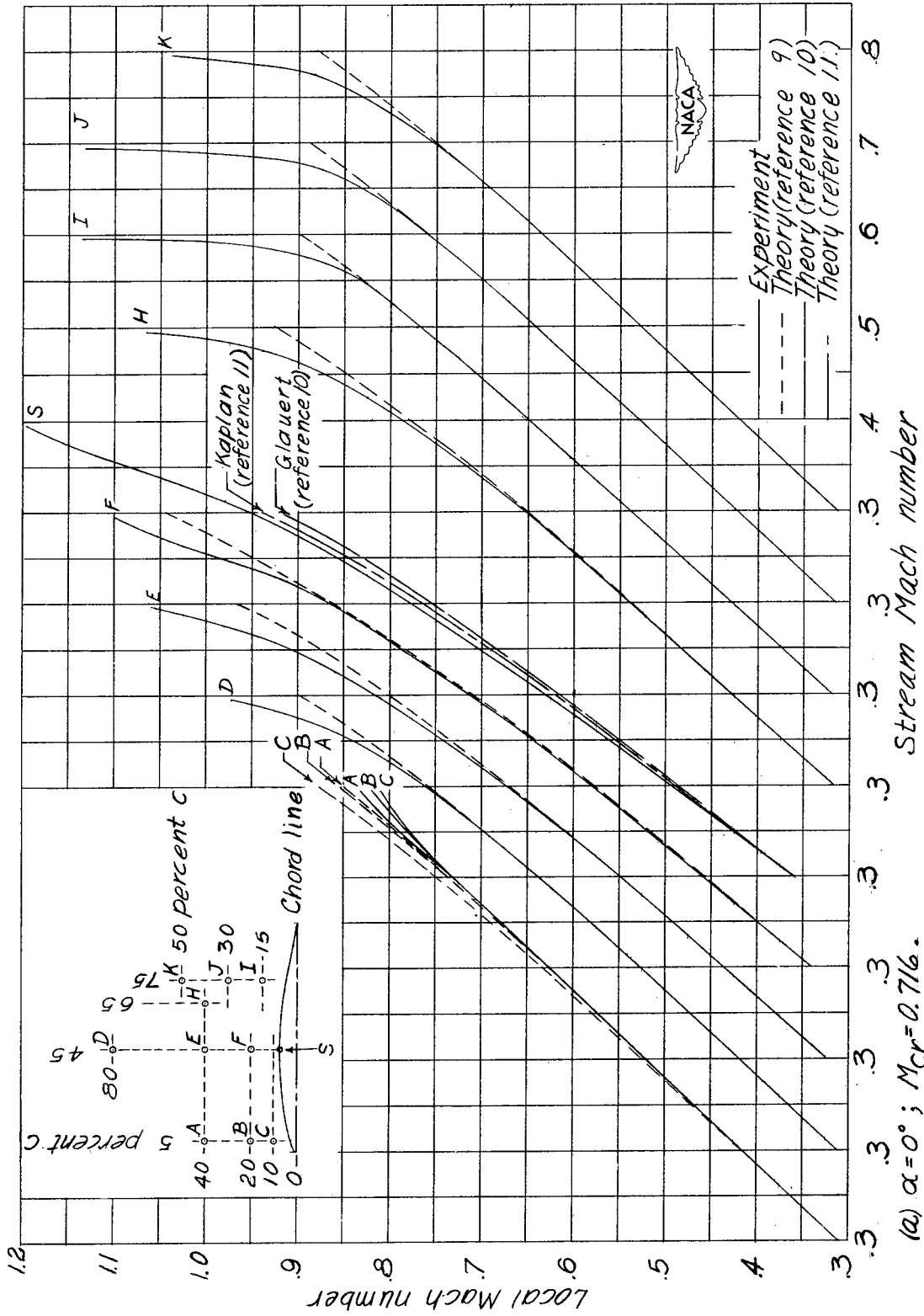
Figure 10.— Concluded.
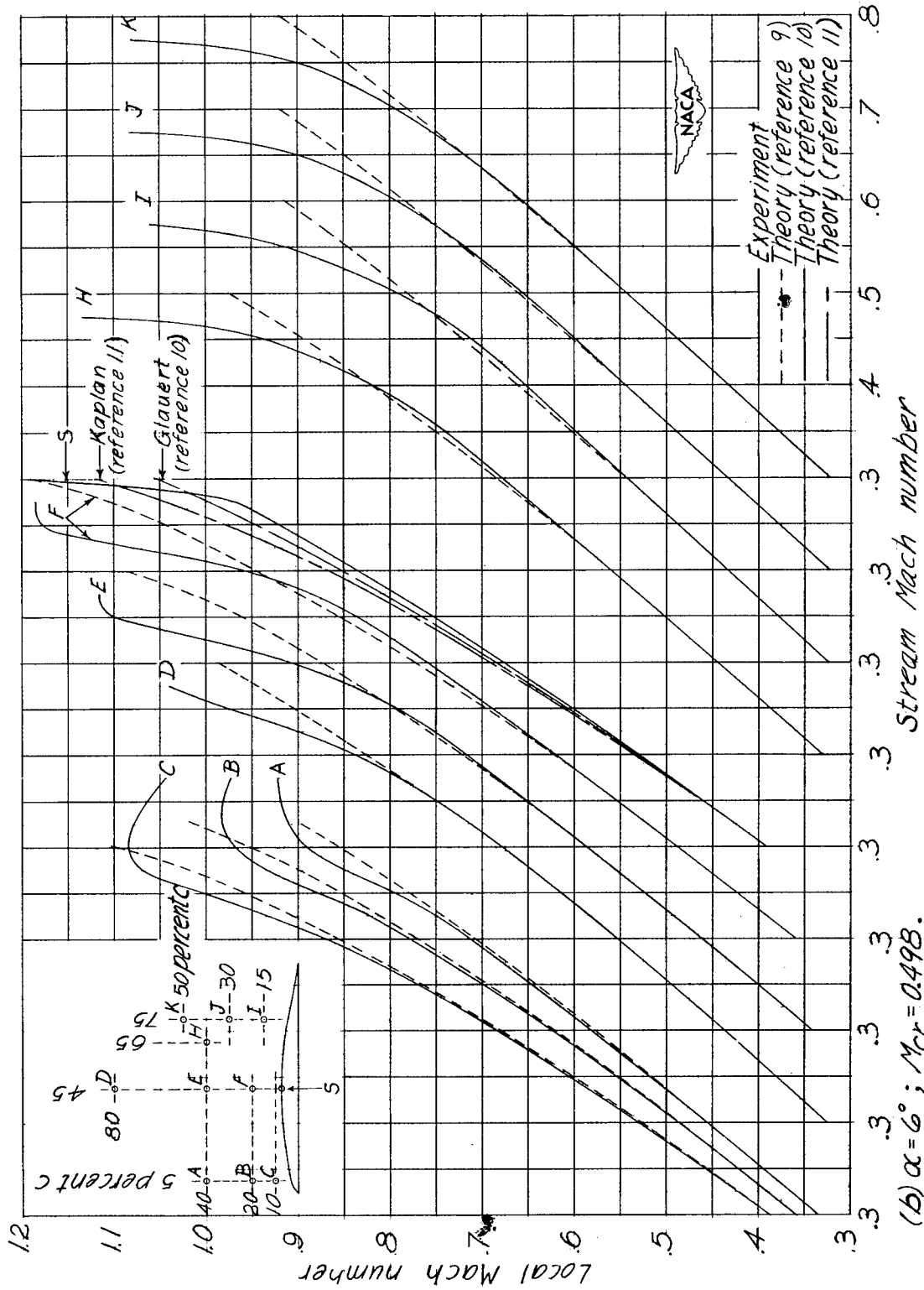
(a) Pressure coefficient contours.

(b) Decay of pressure coefficient
in the flow field.

Figure 11.— Comparison of theoretical with experi-
mental pressure coefficient corrected to M=0
by the method of reference 9.   NACA 66,2-015
airfoil.

(a) $\alpha = 0°$; $M_{cr} = 0.716$.

Figure 12.–Comparison of theoretical and experimental variations of local Mach number with stream Mach number for the NACA 66,2-015 airfoil.

(b) $\alpha = 6°$; $M_{cr} = 0.498$.

Figure 12.- Concluded.